TESI DI DOTTORATO

UNIVERSITÀ DEGLI STUDI DI NAPOLI "FEDERICO II"
DIPARTIMENTO DI INGEGNERIA ELETTRICA E
TECNOLOGIA DELLE INFORMA-ZIONI

DOTTORATO DI RICERCA IN
INGEGNERIA ELETTRONICA E DELLE
TELECOMUNICAZIONI

MODELLING AND PERFORMANCE ASSESSMENT OF HUMAN REACHING MOVEMENTS FOR DISEASE CLASSIFICATION

LUIGI IUPPARIELLO

Il Coordinatore del Corso di Dottorato
Ch.mo Prof. Daniele Riccio

Il Tutore
Ch.mo Prof. Luigi Paura

Il supervisore
Ch.mo Prof. Mario Cesarelli

a.a. 2014-2015

ACKNOWLEDGMENTS

The thesis dissertation marks the end of a long and eventful journey for which there are many people that I would like to acknowledge for their support along the way.

Above all I would like to acknowledge the sacrifices that my parents made to ensure that I had an excellent education. For this and much more, I am forever in their debt.

I have to thank my Giuly for her endless love and encouragement throughout this entire journey. I am forever in debt with this doctorate during which I met my lovely angel.

I want to express my gratitude for the guidance and continuous support during this three years of Prof. Mario Cesarelli. I have greatly benefited from his wide knowledge and experience.

I would like to thank to Prof. Luigi Paura for the supervision of my work and for giving me the opportunity to face my research topic under different points of view. His contribution to Chapter IV of this thesis was fundamental.

I am very grateful to Prof. Paolo Bifulco and Ing. Maria Romano for giving me the opportunity to attend my PhD and for the continuous supervision of my work. They have always been very supportive and constructive in these three years.
I am also grateful to Mr. Cosmo Furno for his pleasant discussions and for its technical support.

Scientific support during the three years was also provided by Fondazione Salvatore Maugeri in Telese Terme. I thank Ing. Giovanni D'Addio for giving me the opportunity to collaborate with this Institution.

DECLARATION OF AUTHORSHIP

I, **LUIGI IUPPARIELLO**, declare that the thesis entitled
MODELLING AND PERFORMANCE ASSESSMENT OF HUMAN REACHING MOVEMENT FOR DISEASE CLASSIFICATION

and the work presented in the thesis are both my own, and have been generated by me as the result of my own original research. I confirm that:

- this work was done wholly or mainly while in candidature for a research degree at this University;

- where any part of this thesis has previously been submitted for a degree or any other qualification at this University or any other institution, this has been clearly stated;

- where I have consulted the published work of others, this is always clearly attributed; where I have quoted from the work of others, the source is always given. With the exception of such quotations, this thesis is entirely my own work;

- I have acknowledged all main sources of help;

- where the thesis is based on work done by myself jointly with others, I have made clear exactly what was done by others and what I have contributed myself;

- parts of this work have been published as:

L.Iuppariello, G.D'Addio, M.Romano, P.Bifulco ,B.Lanzillo, N.Pappone, M.Cesarelli. Analysis of reaching movements of upper arm in robot-mediated therapy. Submitted on January Advances in Occupational Medicine & Rehabilitation.

Giovanni D'Addio; Luigi Iuppariello; Maria Romano; Paolo Bifulco, Associate Professor; Bernardo Lanzillo; Nicola Pappone; Mario Cesarelli. Effects of proprioceptive stimulation on gait Emg patterns in hemiparetic subjects. Submitted on 9 January at Journal of Electromyography and Kinesiology.

L. Iuppariello, M. Romano, G. D'Addio, P. Bifulco, M. Cesarelli. Submovements composition and quality assessment of reaching movements in subjects with Parkinson's Disease. (2015) under second revision by IEEE MeMeA 2015.

Iuppariello L, Romano M., D'Addio G, Bifulco P., Pappone N, Cesarelli M. Comparison of measured and predicted reaching movements with a robotic rehabilitation device (2014) IEEE MeMeA 2014; Lisbon; Portugal; 11 June 2014 through 12 June 2014.

L.Iuppariello, G.D'Addio, P.Bifulco, G.Faiella, B.Lanzillo, N.Pappone, M. Cesarelli Kinematic evaluation of horizontal reaching movements in rotator cuff disease during robotic rehabilitation. (2014) 20th IMEKO TC4 Symposium on Measurements of Electrical Quantities: Research on Electrical and Electronic Measurement for the Economic Upturn, Together with 18th TC4 International Workshop on ADC and DCA Modeling and Testing, IWADC 2014, pp. 856-861.

L. Iuppariello, G. D'Addio, N. Pappone, B. Lanzillo, P. Bifulco, M. Romano, M. Cesarelli Emg patterns of upper arm muscles during robotic rehabilitation 1s t Clinical Movement Analysis World Conference, ESMAC 2014.

L. Iuppariello, M. Romano, G. D'Addio, G. Faiella, P. Bifulco, M. Cesarelli Smoothness evaluation of horizontal reaching movements during robotic rehabilitation 25-27 June, 2014. IV National Conference GNB.

D'Addio, G., Iuppariello, L., Romano, M., Lullo, F., Pappone, N., Cesarelli, M. Kinematic indexes' reproducibility of horizontal reaching movements (2014) IFMBE Proceedings, 41, pp. 81-84.

D'Addio, G., Lullo, F., Pappone, N., Romano, M., Iuppariello, L., Cesarelli, M., Bifulco, P. Relationships of kinematics indexes with amplitude and velocity of upper arm reaching movement. (2013) MeMeA 2013 - IEEE International Symposium on Medical Measurements and Applications, Proceedings, art. no. 6549719, pp. 120-123.

D'Addio G., Iuppariello L., Gallo F, Bifulco P, Cesarelli M., Lanzillo B Comparison between clinical and instrumental assessing using Wii Fit system on balance control. IEEE MeMeA 2014; Lisbon; Portugal; 11 June 2014 through 12 June 2014..

M.Romano, G.D'Addio, L.Iuppariello, P.Bifulco, B.Lanzillo, N.Pappone, M.Cesarelli Quantitative assessment of the EMG patterns of upper arm muscles during robotic rehabilitation. (2014) 20th IMEKO TC4 Symposium on Measurements of Electrical Quantities: Research on Electrical and Electronic Measurement for the Economic Upturn, Together with 18th TC4 International Workshop on ADC and DCA Modeling and Testing, IWADC 2014, pp. 856-861.
G. D'Addio, B. Lanzillo, N. Pappone, L. Iuppariello, G. Matarazzo, F. Lullo, F. Gallo, P. Bifulco, M. Cesarelli, Effects of proprioceptive stimulation on gait EMG patterns in neurological patients SIAMOC 2013.

G. D'Addio, L. Iuppariello, M.Romano, F. Lullo, N. Pappone and M. Cesarelli Kinematic indexes' reproducibility of horizontal reaching movements SIAMOC 2013.

G.D'Addio, L.Iuppariello, M.Romano, P.Bifulco, N.Pappone, B.Lanzillo, M.Cesarelli Effects of Regent Suit on Lower Limb Electromyographic Patterns of hemiparetic subjects. (2014) 20th IMEKO TC4 Symposium on Measurements of Electrical Quantities: Research on Electrical and Electronic Measurement for the Economic Upturn, Together with 18th TC4 International Workshop on ADC and DCA Modeling and Testing, IWADC 2014, pp. 856-861.

Abstract

Human arm motor control has been object of great investigation for several decades, during which some issues have been identified as themes of high interest. There is a wide number of studies on human motor control supporting the theory that reaching and pointing movements are the result of sequences of discrete motion units, called sub-movements. Evidence for the existence of discrete sub-movements underlying continuous human movement has motivated many attempts to "extract" them. Moreover, to analyze the strategy of the reaching movements, gained a great appeal in the rehabilitation field. In fact, understanding movement deficits following central nervous system lesions and the relationships between these deficits and functional ability, is fundamental to the development of successful rehabilitation therapies. The goal of sub-movement extraction is to infer the sub-movement composition of a movement from kinematic data. In the tangential velocity domain, a sub-movement is represented as a uni-modal, bell-shaped function. Determining the number, relative timing, and amplitude of sub-movements that most closely reproduce the original tangential velocity data is a non-linear optimization problem difficult to solve. The experimental observations suggest that sub-movements are ubiquitous but proof of their existence and detailed quantification of their form have been elusive. Although several sub-movement extraction algorithms have been proposed previously, all of them are subject to finding local, rather than global, minima and to producing spurious decomposition results. The first section of this thesis, propose a review on the decomposition methods developed until now and the several methodologies used to extract them. Furthermore, an hybrid sub-movement decomposition method is proposed, based on a robust expectation maximization (EM) constrained algorithm and a scale-space approach capable to overcome the limitations of the EM algorithm, which is a local maximum seeker.

This representation allowed to explore whether the movements are built up of elementary kinematic units by decomposing each surface into a weighted combination of Gaussian functions.
Finally, is proposed a new kinematic and electromyographic assessment of robot assisted upper arm reaching in hemiparetic subjects applying successfully the sub-movement decomposition method implemented to carefully analyze their motor and muscle strategy.

Tables of Contents

LIST OF FIGURES AND TABLES

Chapter 1

Principles of motor control

Human arm motor control has been object of great investigation for several decades, during which some issues have been identified as themes of high interest. Among these are problems such as planning, execution and learning. This chapter addresses the main paradigms that have been used in modeling human arm movement control, and details the models that resulted from each approach.

1.1 Biological motor control

Movement of primates is the result of information processing in a complex hierarchy of motor centers within the nervous system, which yields three levels of control: the spinal cord, brain stem, and motor cortex (Kandel et al, 2000). The highest levels of cortical motor control are often associated with the premotor regions, which are the lateral ventral cortex, the dorsal premotor cortex and the supplementary motor areas. The lowest cortical level is occupied by the primary motor cortex. The premotor cortex has a major role in coordinating and planning complex sequences of movements. It integrates sensory information from the posterior parietal cortex with executive inputs from prefrontal lobes. It projects to the primary motor cortex, which directly controls simple movements of the limbs. Both premotor and primary motor cortex project to the brain stem and the spinal cord. The spinal cord is the lowest level of the hierarchical organization that is directly responsible for executing movements

(Kandel et al, 2000). The premotor cortex has a major role in coordinating and planning complex sequences of movements.
It integrates sensory information from the posterior parietal cortex with executive inputs from prefrontal lobes. It projects to the primary motor cortex, which directly controls simple movements of the limbs. Both premotor and primary motor cortex project to the brain stem and the spinal cord. The spinal cord is the lowest level of the hierarchical organization that is directly responsible for executing movements (Kandel et al, 2000). Human arm motor control has been a subject of investigation for several decades, during which some issues have been identified as themes of high interest (Flash et al, 2001). Among these are problems such as planning, execution and learning. In a broad sense, the motor control problem can be stated as the generation of the muscle activations that best fit the purpose of a movement or manipulation task, given the proprioceptive and external world information available through the body sensors.

1.2 Optimization theory in motor control

Optimization theory has become an important research tool in attempts to discover organizing principles that guide the generation of goal-directed motor behavior. It provides a convenient way to formulate a coarse-grained model of the underlying neural computation, without requiring specific details of the way those computations are carried out. Generally speaking, this application of optimization theory consists of defining an objective function that quantifies what is to be regarded as optimum (i.e., best) performance and then applying the tools of variational calculus to identify the specific behavior that achieves that optimum. This forces us to make explicit, quantitative hypotheses about the goals of motor actions and allows us to articulate how those goals relate to observable behavior. Not all motor behaviors are necessarily optimal but attempts to identify optimization principles can be useful for developing a taxonomy of the complex motor behavior and gaining insight into the

neural processes that produce motor behavior. The complexity of the motor control problem is strongly due to the redundancy of the human motor system as well as the redundant nature of movement tasks.
Many optimization-based models in the literature have been developed to address the "excess degrees-of-freedom" problem.

"How does the motor system select the behavior it uses from the infinite number of possibilities open to it?"

In mathematical parlance, this is an "ill-posed" problem in the sense that many solutions are possible. Even in a simple task such as reaching a target in free space, a multitude of possible solutions are available, each one being a path that takes the hand from the initial to the final position. Infinite solutions exist not only for this path but also for the velocity profile used to track it (Figure 1).

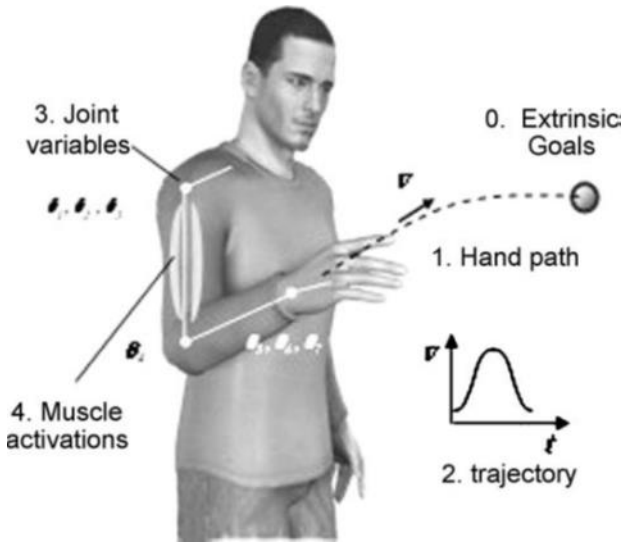

Figure 1. Multiple spaces at which an arm movement is specified.

The freedom to choose both the path and the velocity profile defines the underlying redundancy in a movement task. However, redundancy arises not only in the nature of movement tasks but also as an intrinsic and beneficial feature of the human body, which provides for more flexibility to carry out complex tasks.

One aspect of this redundancy results from the 7 degrees of freedom (DOF) of the kinematic structure of the human arm, which exceeds the minimum necessary number (6 DOF) to move the hand in the three dimensional space (Gui-gon et al, 2007).
The problem of kinematic redundancy was first pointed out by Bernstei (Bernstein, 1967), and labeled the DOF problem.
In the perspective of computational model-ing, the kinematic redundancy is viewed as a problem since most hand positions can be achieved by infinite combinations of the joints.
The number of possible solutions for move-ment planning increases further if muscle commands are considered as an additional variable to be predicted by the theoretical models for motor planning. In fact, due to the muscle configuration in human arm, several muscles are involved in each joint movement and, therefore, it is possible to imagine different combinations of muscle activations that produce the same torque (Wolpert, 1997).
These redundancy issues define sub-problems in motor control theories that are interrelated according to a hierarchy as depicted in Figure 2.

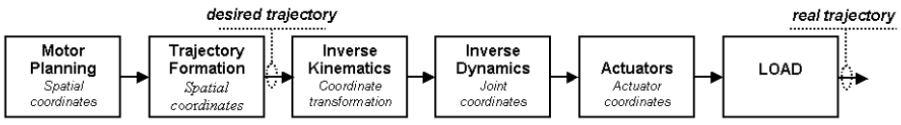

Figure 2. Hierarchical levels of specification for a movement.

Even though the structure of this hierarchy is consensual, the sequence by which sub-problems are solved is conceived differently by different models. Some trajectory formation models postulate that the different levels of redundancy can be solved independently and usually focus only on the hand trajectory planning. Other models are formulated on the basis that these problems are solved interactively and simultaneously. This difference defines the first major line separating motor control theories, as stated by Todorov (Torodov et al, 1998).

Since the former theories ignore the musculoskeletal system that is under control, it is accepted that these cannot aim at explaining completely the underlying biologic principles that give rise to the apparent behavior. Instead they have the less ambitious goal of providing algorithms which produce trajectories that fit well with the observed behavior. These theories can therefore be called Descriptive Models.
The latter theories provide computational models which embody all the fundamental processes carried out by the CNS (Central Nervous System) to produce movement. These models can be assigned the label Complete Models.

1.3 Optimization theory in motor control

In spite of the complexity that the number of redundancy levels suggests, humans show amazingly regularities when generating movement. The strong experimental evidence for such regularities has led researchers to believe that one unifying principle might be used by humans to resolve redundancy and would underlie the observed consistency in behavior. The history of motor control research as therefore been marked by a search for this unifying principle. Early research has focused directly on the kinematic regularities, developing theories that were expressed in terms of the kinematic variables and therefore fall under the Descriptive Models class. Although they showed high predictive accuracy in free movement, these models were weak in accounting for tasks where external forces were present.
However, if a kinematic objective function can be found that leads to optimal trajectories that accurately reproduce the patterns of observed behavior, it implies that the brain ignores non-kinematic factors in selecting and producing that behavior. Nevertheless, a troubling aspect of this theory is that it seems to imply that, at least at the higher levels of the postulated hierarchy, the brain does not take any dynamic considerations into account such as the energy required, the loads on

the limb segments or the force and fatigue limitations of its peripheral neuromuscular system.
To circumvent this problem within the framework of optimization theory, a second type of objective function may be formulated based on dynamic variables (e.g., joint torques, muscle forces, etc., and their time derivatives). If a dynamic objective function can be found that leads to optimal trajectories that accurately reproduce the patterns of observed behavior, it implies that the brain considers dynamic factors in selecting and producing that behavior.
It is also consistent with a theory that neural computations to produce movement are executed in parallel, taking all relevant factors (e.g., dynamics as well as kinematics) into account simultaneously. Hence, this inconsistency in Descriptive Models led researchers to turn to dynamic variables to find a unifying principle that would fit a broader range of movements. In accounting for the dynamics of the arm, these models did address all levels of redundancy, therefore falling under the Complete Models category.
Within this category, the first influential model hypothesized that the minimization of torque change was the principle underlying movement invariants (Uno et al, 1989). Because this and subsequent theories introduced dynamic variables in the optimization procedure, they are known as Dynamic Models.

1.4 Descriptive models

Descriptive models have the purpose of describing the apparent behavior of human motion. Contrarily to Complete models (discussed below), descriptive models do not attempt to mimic the underlying biological principles that give rise to the observed motion features. Instead, these models are computational tools that aim at providing predicted trajectories with a good match with experimental ones.
Among the empirical relations that have been identified in human arm movements are:

- the Fitts law,
- the 2/3 power law,
- the bell shaped velocity profiles in straight movements.

Fitts law concerns rapid, goal directed movements and quantifies the observed and rather intuitive relation that exists between the duration of this kind of movements with the distance and dimension of the target. Mathematically this relation is expressed as follows (MacKenzie, 1991):

$$MT = a + b\log_2\left(\frac{2A}{W}\right)$$

where, MT = movement time, a, b = regression coefficients, A = distance of movement from start to target center and W= width of the target.

The 2/3 power law states that, in curved movements, the velocity (v) is related to the inverse of the curvature radius (k) by the expression:

$$v(t) = \gamma k(t)^{-1/3}$$

where γ is a constant factor which has been experimentally estimated as 0.33. This law basically implies that in curved movements the velocity decreases with increasing curvature. The original form of the power law has the limitation of not being applicable to paths showing straight segments or inflection points (in these cases, velocity goes to infinity). Additionally, the power law is inaccurate at low velocities and cannot predict the velocity reduction at the end of the path (Torodov et al, 1998). One common feature to the subsequent models is the use of optimal control as the strategy to mimic the biologic processes by which human motor control is achieved. It is widely accepted that optimization provides a substantiated framework to explain human motor control because it may reproduce important biological processes, such as learning and natural evolution, that enhance behavior much in the same way as an optimization procedure does (Torodov et al, 2002). The optimal control methodology requires the definition of a cost function, which is based on a quantity that

must be minimized in order to achieve the best performance. The cost function is usually expressed as an integral of that quantity over a period of time. The variables of interest that are used to formulate the cost function define the strategy for trajectory planning.

The bell shaped velocity profile of straight movements is one of the most consistent features of human arm behavior. Flash and Hogan (Flash et al, 1985) presented a model in which the reproduction of bell shaped profiles was a main concern (Figure 3). The authors concluded that considering smoothness of movement as the goal underlying movement control, some apparent features of arm trajectories are explained.

In order to address the optimization of smoothness, a quantitative measure of this property was adopted, which is defined as the derivative of acceleration and named as 'jerk'. Besides the bell shaped velocity profile feature, the model was also motivated by the observation that reaching movements tend to be performed in a straight fashion, regardless of the region in workspace where the movement is performed or its orientation.

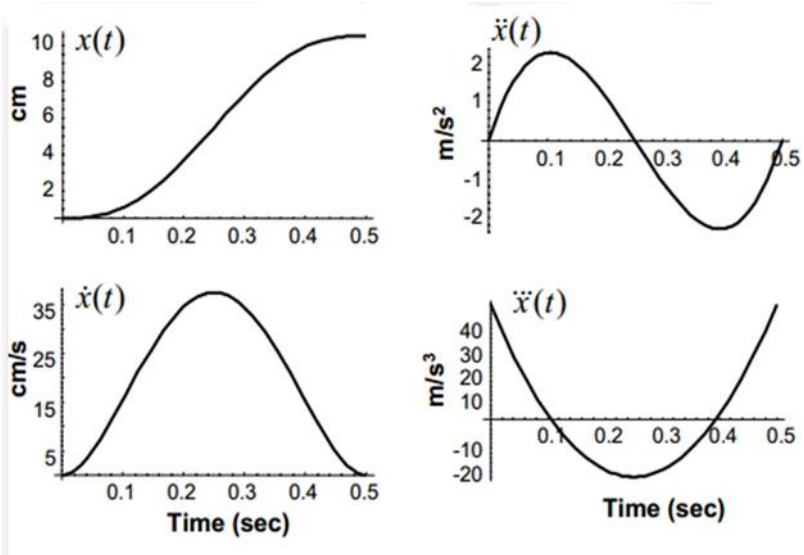

Figure 3. Example of a minimum jerk trajectory.

The fact that these position and velocity features seem to be invariant exclusively when these variables are expressed in hand coordinates (Cartesian space), led the authors to describe minimum jerk in hand coordinates instead of joint coordinates.

For the purpose of addressing planar movements, the magnitude of jerk (J) was defined as follows:

$$J = \sqrt{\left(\frac{d^3x(t)}{dt^3}\right)^2 + \left(\frac{d^3y(t)}{dt^3}\right)^2}$$

where x(t) and y(t) describe the hand position coordinates and a cost function based on the square of that quantity was expressed as:

$$C = \frac{1}{2}\int_0^{t_f}\left(\left(\frac{d^3x(t)}{dt^3}\right)^2 + \left(\frac{d^3y(t)}{dt^3}\right)^2\right)dt$$

where t_f is the time duration.

Optimal control theory was applied to this cost function, subject to the differential equations of movement and several other constraints related to the desired movement.
These constraints are the initial and final positions and also the time duration (t_f) for movement execution. In curved or obstacle avoidance movements, a via-point was also specified. The differential equations of the system are simply the differential relations between position, velocity, acceleration and jerk.
In that study, only planar horizontal movements were addressed namely point-to-point movements and curved unconstrained movements, which could represent obstacle avoidance situations. Applying the optimization procedure to the point-to-point movements, the authors found 5th order polynomials describing both x and y coordinates, which specified a straight line in space with a 4th order polynomial velocity profile.

Concerning the curved movements, two 5th order polynomials were derived for each coordinate, one specifying the trajectory before reaching the via-point and another for the remaining trajectory to the final position. The results of this study were extremely consistent with empirical trajectories, since the predicted point to point movements were straight lines, which is a good approximation of the roughly straight observed paths and the velocity profile is bell shaped as the empirical ones. In this respect, the predicted velocity profiles for curved movements showed a curvature-velocity relation in good agreement with empirical movements. In a practical sense, the minimum-jerk model is very appealing due to its simplicity and the ability to predict the global features of reaching movements. However, this model shows inaccuracy when applied in particular situations, namely curved movements and through point movements (Torodov et al, 1998). Noting that this model may fail to predict the movement path but is accurate in predicting the velocity profile, Todorov and Jordan presented a variation on this model, called constrained minimum jerk model. This model requires that the movement path be predefined and focuses on the generation of the velocity profile. Contrarily to the original minimum jerk model, it does not aim at predicting the path but only the velocity profile. In this aspect, this model is similar to the 2/3 power law, since both predict the velocity, for a given hand path. This model proposes to minimize the following cost function:

$$J = \int_0^{t_f} \left\| \frac{d^3}{dt^3} r[s(t)] \right\|^2 dt$$

where r(s) is the coordinate vector of the path points and s(t) is the distance travelled along the path. According to the given cost function, the purpose of the model is to minimize jerk under the constraint of a path that is pre-defined.

The model was applied to a number of experimental and simulated tasks which evidenced the similarities in speed profiles obtained with

this model and the 2/3 power law. However, this model showed globally better performance and was intrinsically able to deal with the limitations shown by the 2/3 power law.

Commenting on the results of the experiments, the authors mentioned above pointed out the fact that the studied movements were of short duration (1-2 sec) which may have accounted for the good accuracy of the predicted velocities. The authors also remark that the model assumes an implicit relation between path and velocity profile and thus is valid when applied to a particular movement execution but its meaning is lost if applied to an average path of a number of trials.
The above models are concerned strictly with the description of hand trajectories in space, leaving aside the problem of joint trajectories prediction. If these models are used in a complete simulation of the human arm, additional strategies must be employed in order to compute the joints values for each hand position.
This problem has been addressed by different studies, which focus primarily on joint redundancy resolution. Several studies have investigated the hypotheses that joint redundancy might be simplified by *Donders' law* (Marotta et al, 2003). Donders law was formulated to describe the redundancy resolution policy observed in the positioning of the eye.
Donders' law states that any possible vector describing a rotation of the eye cannot occupy an arbitrary position in space; instead it is constrained to lie in a plane. By applying this law, the number of DOF of the eye is reduced from 3 to 2 and any gazing direction is univocally related to a rotation vector of the eye. Due to the similarities of the problems (excess of DOF) and the fact that both the eye and arm are controlled by the CNS, some authors speculated that the same law might also be applicable to the positioning of the arm.
This motivation led to a number of studies which explored the usability of Donders' law in the joint redundancy problem. The reported results indicate that the application of Donders' law in the

arm is limited and that a more complex strategy that is yet to be identified probably is used instead (Marotta et al, 2003). However, in particular tasks it was observed that Donders' law was accurate, which indicated that this law may be a special case of that general strategy.

1.5 Complete Models

The most influential model described in the previous section, the minimum-jerk model, relies on a cost function based on the kinematic variables to find the solution for trajectory planning. Additionally, this model focuses only on the generation of trajectories in Cartesian space, leaving open the question of how joint space redundancy is solved. Complete Models, addressed in this section, comprise theories that consider the arm dynamics and therefore include in the cost function torques and external forces values. As a consequence of dealing with the whole arm dynamics, which is non-linear and depends on joint kinematics, a by-product of the minimization of a cost function is the resolution of all levels of redundancy.

1.6 Dynamic Models

Dynamic models take into account the dynamics of the arm and focus on joint torques, external forces and motor commands (Wolpert, 1997). Three major models were presented and named, according to the variable of interest, as 'minimum torque change', 'minimum motor command change' and 'minimum commanded torque change'. Minimum torque change model, the most influential dynamic model, was presented in Uno et al (Uno et al, 1989). The authors pointed out that kinematic models rely on the improbable assumption of

considering that trajectories depend solely on the initial and final positions, disregarding the physical apparatus to execute them, or the external forces. It has been suggested that movement planning should consider dynamic aspects of the arm and the task which led the authors to test different dynamic variables inside the cost function.

The torque change was accepted as the cost function variable that yields the best agreement with observed behavior. The cost function was defined as:

$$C = \frac{1}{2}\int_0^{t_f} \sum_i \left(\frac{dz_i}{dt}\right)^2 dt$$

where z_i is the torque generated at joint i. This objective function was minimized under the constraints of the musculoskeletal dynamics. For the purpose of addressing planar movements, the authors approximated the arm dynamics by a two-joint planar robot dynamics, with inertial, geometric and viscosity parameters representative of the human arm characteristics. Due to the highly nonlinear nature of this system, it is much more complex to find the unique optimal trajectory in this case than in the kinematic model case, in which the system is described by linear kinematic relations. This difficulty was overcome by employing a computational iterative method to determine the optimal solution. With this method the determination of hand coordinates trajectories involves the computation of the lower level torques at the joints. This is a fundamental implication of dynamic models, in which the three levels of motor control cannot be computed in isolation. Instead, the computation of the hand trajectory is embedded with the lower levels of joint trajectory and joint torque computation. As the output of the movement planning, hand trajectory, joint trajectory and torque are produced simultaneously.

Chapter 2

Composability of the human movement

This chapter focuses on the discretization theory of the arm movement. The segmentation of seemingly continuous movements into segments has been theorized for many years. These segments may be considered as movement "primitives", or building blocks of more complex movements. The existence of these fragments, or sub-movements as they are called, has been supported by a wide range of studies over the past 100 years. Evidence for the existence of discrete sub-movements underlying continuous human movement has motivated many attempts to "extract" them. Recently, the sub-movement theory gained a great appeal in the rehabilitation field. In fact, understanding movement deficits following CNS lesions and the relationships between these deficits and functional ability, is fundamental to the development of successful rehabilitation therapies.

2.1 Motor planning and trajectory formation

Over the past decades, research on sensorimotor control and on trajectory formation has gained momentum as is evident in new journals, conferences, and more highly visible publications. This growth in both fundamental and applied motor neuroscience is partly spurred by applications to rehabilitation, robotics, and brain-machine interfaces. Trajectory Formation is one of the basic functions of the neuro-motor controller, such as the compensation of loads, the pursuit of moving targets, the appropriate control of impacts (e.g. hitting), and the generation of contact forces (e.g. pushing).

In particular, reaching, pointing, avoiding, generating scribbles, drawing, handwriting and gesturing are different motion paradigms which all result in the generation of planar or spatial trajectories of different degrees of complexity.
Further, they require extremely complicated and as yet poorly understood computations such as the encoding of target position, the coordination between the motions of several limb segments and the generation of appropriate muscle patterns [Flash et al,1991]. So, even in a simple task such as reaching a target in free space, a multitude of possible solutions are available, each one being a path that takes the hand from the initial to the final position reach towards a stationary target they do not use the full repertoire of possible trajectories but produce movements with certain invariant kinematic properties, suggesting a tendency to select one trajectory from the many available.

2.2 The sub-movements theory

As discussed above, one robust finding that has emerged from several works [Hogan,1984; Abend et al, 1982; Flash et al, 1985] is that, in the absence of any overriding requirement such as maximum speed or precision, the unimpaired planar reaching motions (or free reaching movements) are characterized by a straight path of the hand movement in the Cartesian space and by a single-peaked, bell-shaped velocity profile. This usually leads to smooth and accurate movements.
However, several studies noted that reaching more complex movements or movements under constraints of time and spatial accuracy are often characterized by irregular and asymmetric multi-peaked velocity profiles. These experimental evidences led to the emergence of the theory of the discretization of the movement.

There is a wide number of studies on human motor control [Gross et al, 2002; Von Hofsten, 1991; Rucci et al, 2007; Rohrer, 2006; Collewijn et al, 1988; Dounskaia et al, 2007; Morasso, 1981; Di Pietro et al, 2009; Flash et al, 1985; Lee et al, 1997] supporting the theory that reaching and pointing movements are the result of sequences of discrete motion units, called sub-movements.

Like primitives in natural and computer languages can be combined to generate a grammar of more complex constructs, the central nervous system can combine these discrete units to generate a manifold of more complex motor behaviors.

Identifying fundamental building blocks that underlie human movement is a major goal of motor control studies. If such a structure could be identified and accurately characterized, it would provide the ability to scrutinize human movement at a deeper level than has been previously possible.

Moreover, considering any movement as a combination of "primitive" blocks leads to interesting theory that lends itself well to a mathematical application, especially for the striking analogy with the Fourier approach. Evoking Fourier's theorem, in fact, it is clear that a wide range of almost-periodic behaviors may be composed by superposition of oscillatory primitives; so, considering the movement as a periodic (or not) signal is a very fitting analogy.

The possibility that observable movements are composed of sub-movements is by no means a new idea since the search for primitive elements that generate actions dates back at least a century. As early as 1899, Woodworth noted that voluntary movements appear to be accomplished as a series of corrective sub-movements [Woodworth, 1989].

Then sub-movements have been observed in a variety of motor tasks, such as handwriting [Morasso et al, 1982], slow finger movements [Vallbo et al, 1993], and elbow cyclical movements [Doeringer et al, 1998] and under a number of experimental conditions, such as visually guided [Milner et al, 1990; Milner et al, 1992; Burdet et al,

1998], blinded [Doeringer et al, 1998], high accuracy [Milner et al, 1992] and low-accuracy [Di Pietro et al, 2004] tasks.

While earlier work assumed sub-movements were made at fixed, non-overlapping intervals [Crossman et al, 1983] or immediately following one another [Meyer et al, 1982; Meyer et al, 1988], later work allowed for the possibility that the sub-movements overlap the primary movement [Flash et al, 1991; Berthier, 1997; Milner et al, 1990; Krebs et al, 1999], so considering these discrete blocks as primitive dynamic elements of motor behavior [Hogan et al, 2002].

The constrained velocity is another variable that leads to the insurgence of sub-movements during a reaching movement. For example, a fast movement to a fixed target can be thought of as being composed of one or more sub-movements, each of which is pre-programmed and generated by an inverse internal model [Shadmehr et al, 2005; Davidson et al, 2000].

The first of these is called the initial, or primary, sub-movement. Then, based upon the output of a forward model and/or visual feedback and accuracy requirements, the primary sub-movement may be modified slightly near the end (allowing for the delay in the motor control system), corrective sub-movements may be made before the end of the primary sub-movement (concurrent/ overlapping sub-movements), or after the primary sub-movement (discrete/non-overlapping sub-movements).

These corrective sub-movements cause a deviation from the typical bell-shaped velocity profile of a unconstrained movement [Morasso 1981; Hogan, 1984]. This means that, despite humans seems to have little difficulty in moving accurately to a desired position, the accuracy declines as movement speed increases [Woodworth, 1899].

2.3 The sub-movements in the rehabilitation process

Over the last years, the sub-movement theory gained a great appeal in the rehabilitation field. Understanding movement deficits following CNS lesions and the relationships between these deficits and functional ability, is fundamental to the development of successful rehabilitation therapies [Lough et al, 1984]. When a subject with spinal cord or orthopedic injury perform a reaching movement, the resulting movement differs from that performed by a person with an intact nervous system. particularly.

Damage to areas that contribute to the execution of smooth, coordinated movement may result in some type of impairment in the quality of the movement. The symptoms most often displayed involve an incorrect timing of muscle activation [Carr et al, 1987], the addition of involuntary movement as result of the muscle firing spontaneously, a lower accuracy of the movement and the occurrence of a pathological synergy as compensatory strategy of the motor deficit [Gowland et al, 1992; Trombly, 1992; Levin, 1996].

Krebs [Krebs et al, 1999] observed that movements performed by subjects in the early stage of stroke recovery were fragmented and highly stereotyped in their shapes. Decomposing movements into individual components should reveal the strategy that is used by the pathological subjects to perform a motor task. He reported that movements made by patients recovering from stroke become smoother as recovery proceeds and this was attributed to a progressive overlapping and blending of sub-movements.

Subsequently, progressive changes in sub-movements were again proposed as the mechanism underlying progressive changes in movement smoothness during motor recovery from stroke and, more in general, as a process that characterizes motor recovery from stroke (Rohrer et al., 2002; Di Pietro et al, 2009).

Chapter 3

Models for the sub-movements decomposition

The goal of sub-movement extraction is to infer the sub-movement composition of a movement from kinematic data. In the tangential velocity domain, a sub-movement is represented as a uni-modal, bell-shaped function.
Determining the number, relative timing, and amplitude of sub-movements that most closely reproduce the original tangential velocity data is a non-linear optimization problem difficult to solve. In this chapter, at first, formally define optimization problems and identify the principle classes of problems. Particularly are summarized the characteristics of nonlinear optimization problems and solution methods.
Then, is reported a review on the decomposition methods developed until now and the several methodologies used to extract them. Furthermore, is proposed a novel sub-movement decomposition method based on a EM constrained algorithm.
This representation allowed us to explore whether the movements are built up of elementary kinematic units by decomposing each surface into a weighted combination of Gaussian functions. These can be used to examine underlying principles of movement generation during the execution of a reaching movement.

3.1 The optimization problems

Many application problems in engineering decision sciences and operations research are formulated as optimization problems. Optimization problems (Figure 4) are made up of three basic components:

- a set of unknowns or ***variables***, which can take on continuous, discrete, or symbolic values;
- an ***objective function*** to be minimized or maximized, which can be continuous or discrete and have linear or nonlinear forms.
- a set of **constraints** that specify feasible values of the variables. The constraints can also have linear or nonlinear forms, can be defined implicitly or explicitly or may not even exist.

The optimization problem entails *"finding values of the variables that optimize (minimize or maximize) the objective function while satisfying the constraints",*

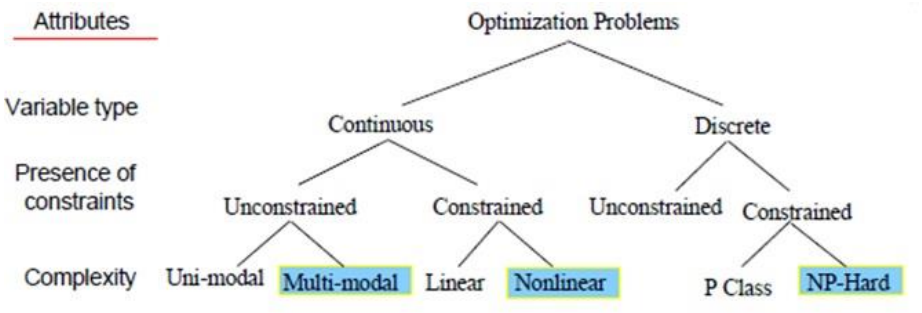

Figure 1. A classification of the optimization problems.

A general minimization problem is defined as follows:

Given a set *D* and a function (the *objective function*) $f : D \rightarrow P$, find at least one point $x^* \in D$ that satisfies $f(x^*) \leq f(x)$ for all $x \in D$, or show the non-existence of such a point.

A mathematical formulation of a minimization problem is as follows:

$$\text{minimize } f(x) \qquad (1.1)$$

$$\text{subject to } x \in D.$$

In this formulation $x = \{x_1, x_2, \ldots\ldots, x_n\}$ is an n-dimensional vector of unknowns (or variables). The function *f* is the *objective function* of the problem, and *D* is the feasible domain of x specified by *constraints*. The codomain P of an objective function as well as its range must be a subset of the real numbers ($P \subseteq R$),

Definition 1.1 (Global Minimum). A vector, $x^* \in D$, satisfying $f(x^*) \leq f(x)$ for all $x \in D$ is called *global minimizer* of *f* over *D*. The corresponding value of *f* is called a *global minimum*.

Definition 1.2 (Local Minimum). A vector $x^* \in D$ is called a local minimizer of *f* over *D* if $f(x^*) \leq f(x)$ for all $x \in D$ close to x^*. The corresponding value of *f* is called a *local minimum.*

Note that since $\max f(D) = - \min(- f(D))$, maximization problems can be transformed into minimization problems shown in (1.1).

Definition 1.3 (Global Optimum). A global optimum $x^\star \in D$ of one (objective) function

$f : D \rightarrow R$ is either a global maximum or a global minimum.

Even a one-dimensional function $f : D \rightarrow P$ may have more than one global maximum, multiple global minima, or even both in its domain X (Figure 5). The correct solution of such an optimization problem would then be a set D^* of all optimal inputs in D rather than a single maximum or minimum. Furthermore, the exact meaning of optimal is problem dependent. In single-objective optimization, it either means minimum or maximum.

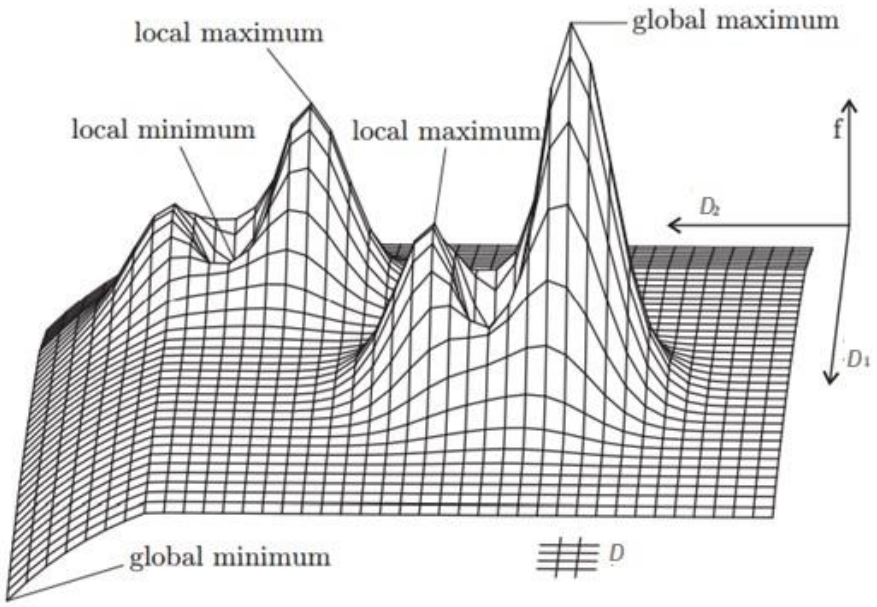

Figure 2. Global and local optima of a two-dimensional function.

3.1.1 Continuous optimization problems

Optimization problems are classified into *continuous* and *discrete* problems. A problem is continuous if the unknowns (variables) take on continuous real values, i.e., D in (1.1) consists of real numbers.

A problem is discrete if the unknowns take on discrete, usually integer values.

Continuous optimization problems are further classified into *constrained optimization* and *unconstrained optimization* based on the presence of constraints. Problems without constraints fall into the class of unconstrained optimization.

$$\text{minimize } f(x) \qquad (1.2)$$

$$\text{subject to } x \in R^n.$$

There are two types of optimal points of an optimization problem: local minima and global minima. A local minimum has the smallest value in a local feasible region surrounding itself, whereas a global minimum has the smallest value in the whole feasible domain. In a continuous unconstrained optimization problem, an objective function is minimized in the real domain. An unconstrained optimization problem is *uni-modal* if its objective function is convex. A uni-modal problem has *only one* local minimum, which is the global minimum at the same time. Uni-modal problems are relatively easy to solve. They have been studied extensively for decades. Many algorithms have been developed, including gradient descent, Newton's method, quasi Newton's methods, and conjugate gradient methods. These algorithms are very efficient and can solve optimization problems with tens of thousands of variables within seconds.

A problem is *multi-modal* if its objective function has *more than one* local minimum. General non-linear functions are multi-modal and may have many local minima that are not global minima. Multi-modal problems are much more difficult and yet plentiful in real applications. Although many methods have been developed for multi-modal problems, most of them are efficient only for subclasses of problems with specific characteristics. Methods for general multi-modal problems are far from optimal.

When each dimension of D in (1.1) consists of real values constrained by simple lower and/or upper bounds, the corresponding optimization problem is called a *simple-bounded continuous optimization problem*.

$$\text{minimize } f(x) \qquad (1.3)$$

$$\text{subject to } l \le x \le u$$

$$x \in R^n.$$

where l and u are constants.

We put simple-bounded constrained problems in the class of unconstrained optimization because simple-bound constraints (for example $1 \le x \le 5$) are easy to handle, and algorithms for problems without constraints and with simple-bound constraints are similar. The remaining problems with nontrivial constraints belong to the class of constrained optimization.

As shown in Figure 4 constrained continuous problems are classified into linear and non-linear depending on the form of constraint functions. When D in (1.1) is bounded by linear functions, the corresponding optimization problem is called a *linear constrained problem*. This class of problems is relatively easy to solve. Among these problems, two types of problems that have been studied extensively and solved well are *linear programming* and *quadratic programming* problems. Efficient algorithms have been developed to solve them very well [Dantzig G. B., 1963; Floudas et al, 1995].

When D is characterized by non-linear functions, the optimization problem is called a *non-linear optimization* or a *non-linear programming problem*.

$$\begin{aligned} &\text{minimize} && f(x) && (1.4)\\ &\text{subject to} && h(x) = 0 \\ & && g(x) \le 0 \\ & && x \in R^n. \end{aligned}$$

where h(x) represents a set of equality constraints and g(x) a set of inequality constraints. In a nonlinear optimization problem, the objective function as well as the constraint functions are nonlinear. Nonlinear constrained problems are difficult to solve because nonlinear constraints may constitute feasible regions that are difficult to find, and nonlinear objectives may have *many local minima*. Many application problems fall into this class [Flaudas et al, 1990; Horst et al, 1995].

3.1.2 Discrete optimization problems

When the feasible set D in (1.1) consists of discrete values, the problem is called a *discrete optimization problem*. Discrete optimization is a field of study in combinatory_ as well as in mathematical programming. A classification of combinatorial problems consists of four categories: a) evaluation of required arrangements, b) enumeration of counting of possible arrangements, c) extremization of some measure over arrangements, and d) existence of specific arrangements [Parlos et al, 1988] Discrete optimization usually refers to the third category.

Some famous examples of discrete optimization problems are as follows:

- *Knapsack Problem.* Determine a set of integer values x_i , i=1, 2, ……., n, that minimize $f(x_1, x_2,\ldots\ldots,x_n)$ subject to the restriction $g(x_1, x_2,\ldots\ldots,x_n) \geq b$ where b is a constant.
- *Traveling Salesman Problem.* Given a graph (directed or undirected) with specified weights on its edges, determine a tour that visits every vertex of the graph exactly once and that has minimum total weight.

- *Bin Packing.* Given a set of weights, w_i, $1 \leq i \leq n$ and a set of bins, each with fixed capacity W, find a feasible assignment of weights to bins that minimizes the total number of bins used.

Discrete optimization problems, including the above examples, can be expressed in the following integer programming (IP) formulation:

$$\begin{aligned} \text{minimize} \quad & f(x) \qquad (1.5) \\ \text{subject to} \quad & h(x) = 0 \\ & g(x) \leq 0 \\ & x \in I^n \end{aligned}$$

where I represents the integer space. Variable domain D consists of integers and is characterized by equality constraints h(x) and inequality constraints g(x).
Notice the similarity of (1.5) to the formulation of continuous constrained optimization problem in (1.4).
As shown in Figure 4, the discrete optimization problems are classified according to the existence of constraints and their computational complexity.
When there is no constraint besides integral requirements of variables, the problem is called an *unconstrained problem*.
With additional constraints, the problem is called a *constrained problem*. An unconstrained *discrete optimization problem* has the following form:

$$\text{minimize } f(x) \qquad (1.6)$$

$$\text{subject to } x \in I^n.$$

When D consists of integer values constrained by simple lower and/or upper bounds, the optimization problem is called a *simple-bounded discrete optimization problem:*

$$\text{minimize } f(x) \qquad (1.7)$$

$$\text{subject to } \quad l \leq x \leq u$$

$$x \in I^n.$$

As in the continuous case, we associate simple-bounded discrete optimization problems with the class of unconstrained problems. Algorithms for these problems are similar. The majority of discrete optimization problems have some constraints, and few are unconstrained optimization problems.

When domain D and objective *f* are characterized by linear functions, the optimization problem is called an *integer linear programming (ILP) problem.*

An example of ILP problems is the following inequality-form knapsack problem:

$$\text{minimize } \sum_{i=1}^{n} c_i x_i$$

$$\text{subject to } \sum_{i=1}^{n} a_i x_i \geq b_j$$

$x_i = 0$ or 1, a_i and c_i are integers $\quad i = 1, 2, \ldots\ldots, n$

Discrete constrained optimization problems have been studied extensively in computer science and operations research. Based on their computational complexity, there are two important classes of discrete optimization problems: *Class P* and *Class NP*. Class P contains all problems that can be solved by algorithms of polynomial-time complexity, where P stands for polynomial. Examples of Class P problems are matching, spanning trees, network flows, and shortest path problems. Class P problems have been well studied. Many

discrete problems in real-world applications do not have polynomial-time algorithms and are more difficult to solve than those in Class P. Among them, one important class is NP. Class NP includes all those problems that are solvable in polynomial time if correct polynomial-length guesses are provided. Examples are knapsack, traveling-salesman, and bin-packing problems. Problems to which all members of NP polynomially reduce are called *NP-hard*. The Class NP contains the Class P as well as a great many problems not belonging to P.

3.1.3 Challenges in solving non-linear optimization problems

Except for trivial cases, nonlinear optimization problems do not have closed-form solutions and cannot be solved analytically. Numerical methods have been developed to search for optimal solutions of these problems. The process of solving an optimization problem becomes a process of searching for optimal solutions in the corresponding search space. *Finding global minima of a nonlinear optimization problem is a challenging task*. Non-linear constraints form feasible regions that are hard to find and difficult to deal with, and nonlinear objectives have many local minima that make global minima hard to find and verify.

In solving nonlinear constrained optimization problems, there may not be enough time to find a feasible solution when nonlinear constraints constitute small feasible regions that are difficult to locate.

Second, nonlinear objective functions in both constrained and unconstrained optimization problems make global minima difficult to find. Figure 6 illustrates the challenges of a multi-modal nonlinear function. The terrains have different characteristics and cause problems for search algorithms that adapt to only a subset of the characteristics.

Because of large slopes, tall hills are difficult to overcome in gradient-based search methods. In the search space, gradients can vary many orders of magnitude, which make the selection of appropriate step-size difficult. Large shallow basins and flat plateaus provide little information for search direction, and may take a long time for a search by algorithm to pass these regions if the step-sizeis small. Further, small local minima are difficult to find.

Figure 3. Illustration of difficulties in optimizing a nonlinear function. There may exist local minima in a multi-modal nonlinear function with different characteristics, shallow or deep, wide or narrow.

These difficulties happen in the extraction problem of the sub-movements in a reaching movements as shown in the section 3.3. In nonlinear optimization problems, global optimal solutions are not only difficult to find, but also difficult to verify. There is no local criterion for deciding whether a local optimal solution is a global optimum. Therefore, nonlinear optimization methods cannot guarantee solution qualities for general nonlinear problems.

To summarize, the challenges of general nonlinear optimization include the following:

- Feasible regions bounded by nonlinear constraints may be difficult to find;
- The objective-function terrain of search space may be very rugged with many sub-optima;

- There may exist terrains with large shallow basins and small but deep basins;
- The dimension of optimization problems is large in many interesting applications;

The objective and constraints are expensive to evaluate.

3.1.4 Characteristics of non-linear optimization algorithms

A large number of optimization methods have been developed to solve nonlinear optimization problems. Nonlinear optimization methods are classified into local optimization and global optimization methods. Global optimization methods have the ability to find global optimal solutions given long enough time, while local optimization methods do not.

Local optimization methods include gradient descent, Newton's method, quasi Newton's method, and conjugate gradient methods [Arrow et al, 1958; Baldi, 1995; Gorse et al, 1992; Kinsella, 1992; Sturua et al, 1991].

They converge to a local minimum from some initial points. Such a local minimum is globally optimal only when the objective is quasi-convex and the feasible region is convex, which rarely happens in practice. For nonlinear optimization problems, a local minimum can be much worse than the global minimum.

To overcome local minima and search for global minima, global optimization methods have been developed.

Global optimization methods look for globally optimal solutions [Floudas et al, 1990; Horst et al, 1993; Pardalos et al, 1987]. As stated by Griewank [Griewank, 1981], global optimization for nonlinear problems is mathematically ill-posed in the sense that a lower bound for the global optima of the objective function cannot be given after any finite number of evaluations of the objective function, unless the

objective satisfies certain conditions, such as the Lipschitz condition, and the search space is bounded.

Global optimization methods perform global and local searches in regions of attraction and balancing the computation between global and local exploration. A global search method has the mechanism to escape from local minima, while a local search method does not. In an optimization problem, a region of attraction defines the region inside which there is a local minimum and the constraints are satisfied.

The regions of attraction trap local search methods. In the general black-box model, global optimization is performed without a priori knowledge of the terrain defined by the objective and the constraints. Therefore, global optimization algorithms use heuristic global measures to search for new regions of attraction. Promising regions identified are further optimized by local refinement procedures, such as gradient descent and Newton's methods. In many real-world applications, the computational complexity of finding global optima is prohibitive. Global optimization methods usually resort to finding good sub-optimal solutions.

Nonlinear optimization methods employ various search algorithms to escape from local minima and search for global optima. The characteristics of search algorithms are summarized as follows:

a) Representation of search space. A search space specifies the range of variable assignments that are probed during the process of searching for optimal solutions. The search space may contain only feasible regions specified by constraints, or may contain some infeasible regions as well. The search space of an optimization problem can be finite or infinite, which directly affects the computational complexity of the corresponding search algorithms.

b) Decomposition strategies. Some search algorithms work on the whole search space directly, while others decompose the large search space into smaller ones and then work on them separately. Divide-and-conquer and branch and bound are two decom-position strategies

that have been applied in many search algorithms for both continuous and discrete problems.

c) Heuristic predictor or direction finder. During a search process, search algorithms have used many different heuristics to guide the search to globally optimal solutions. In branch and bound methods, heuristic lower bounds are associated with decomposed smaller sub-spaces to indicate their goodness. For example, in interval methods, interval analyses are used to estimate the lower bounds of a continuous region. Similarly, in solving integer programming problems, discrete problems are relaxed into continuous linear programming problems to obtain a lower bound. The lower-bound information is further used to guide the search. In simulated annealing, the objective values of neighborhood points provide a direction for the search to proceed.

In genetic algorithms, search directions are obtained from fitness values of individuals in a population. Components of individuals with high fitness are reinforced, and the search moves in directions formed by good building blocks.

d) Mechanisms to help escape from local minima. To find globally optimal solutions, a search algorithm has to be able to escape from local minima. Probabilistic methods get out of local minima based on probabilistic decisions. For example, simulated annealing methods can move in a direction with worse solutions using adaptive probabilities. Genetic algorithms escape from local minima through probabilistic recombination of individuals and random perturbation of existing solutions.

e) Mechanisms to handle constraints. To solve constrained optimization problems search algorithms have to handle constraints efficiently.

f) Stopping conditions. Some optimization problems can be solved optimally in a short amount of time. Unfortunately, most real-world applications are large and have high computational complexity, which makes optimal solutions impossible to find or verify. Hence, search algorithms have to terminate in a reasonable amount of time and settle on approximation solutions. The degree of approximation is usually proportional to the amount of time available. Better solutions can be found given more execution time.

3.1.5 Overcoming local minima

General nonlinear optimization problems are difficult to solve due to the large number of local minima in the search space. Local minima of nonlinear objective functions make local searches more difficult.
Search methods that are trapped by local minima are incapable of obtaining good solutions. The mechanism of escaping from local minima determines the efficiency of a global search algorithm and the solution quality it obtains, and has long been the central issue in developing global search methods.
As discussed above, solution methods for nonlinear optimization problems can be classified into local and global methods.
Local optimization methods, such as gradient descent and Newton's methods, use local information (gradient or Hessian) to perform descents and converge to a local minimum. They can find local minima efficiently and work best in uni-modal problems.
Global methods, in contrast, employ heuristic strategies to look for global minima and do not stop after finding a local minimum.
Note that gradients and Hessians can be used in both local and global methods.

Figure 7 shows a classification of local optimization methods for unconstrained non-linear optimization problems. The methods can be broadly classified as zero-order, first-order, and second-order methods based on the derivative information used during the search. Generally higher-order methods converge to local minima faster.

Zero-order methods do not use derivatives of objective functions during optimization. Examples are the simplex search method, the Hooke and Jeeves method, the Rosenbrock method, and the conjugate direction method.

First-order methods use first-order derivatives of the objective function during the search. Examples are the gradient-descent method, the discrete Newton's method, the quasi-Newton methods, and the conjugate gradient methods.

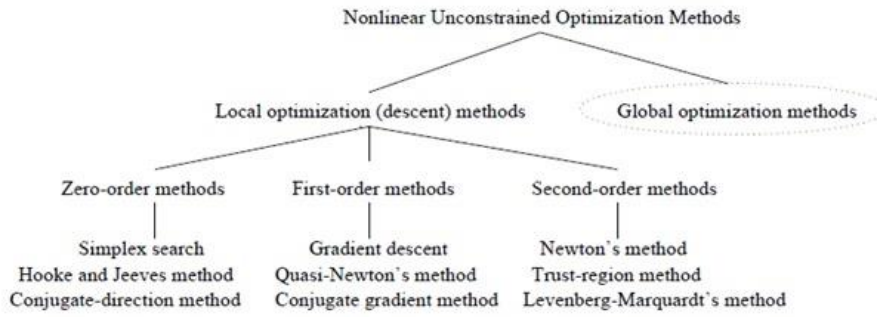

Figure 4. Classification of local optimization methods for unconstrained nonlinear optimization problems.

The gradient-descent method performs a linear search along the direction of the negative gradient of the minimized function.

The discrete Newton's method approximates the Hessian matrix by the finite difference of the gradient.

Quasi-Newton methods approximate the curvature of the nonlinear function using information of the function and its gradient only, and avoid the explicit evaluation of the Hessian matrix.

Conjugate gradient methods combine the current gradient with the gradients of previous iterations and the previous search direction to form the new search direction. They generate search directions without storing a matrix.

Second-order methods make use of second-order derivatives. They include Newton's method, Levenberg-Marquardt's method, and trust region methods. Local optimization methods converge to local minima. For some applications, local optima may be good enough, particularly when the user can draw on his/her own experience and provide a good starting point for local optimization algorithms. However, for man applications, globally optimal or near-optimal solutions are desired. In nonlinear optimization, objective functions are *multi-modal* with many local minima. Local search methods converge to local minima close to the initial points. *Therefore, the solution quality depends heavily on the initial point picked*.

When the objective function is highly nonlinear, local-search methods may return solutions much worse than the global optima when starting from a random initial point.

To overcome the deficiencies in local search methods, global search methods have been developed with global search mechanisms. Global search methods use local search to determine local minima, and focus on bringing the search out of a local minimum once it gets there.

Figure 8 shows a classification of nonlinear global optimization methods. Methods to solve global optimization problems have been classified as either *probabilistic* or *deterministic*. Probabilistic (stochastic) methods evaluate the objective function at randomly sampled points from the solution space. Deterministic methods, on the other hand, involve no element of randomness.

Alternatively, global optimization algorithms can also be classified as reliable and unreliable. Reliable methods guarantee solution quality while unreliable methods do not. Probabilistic methods, including simulated annealing, clustering, and random searching, fall into the unreliable category. Unreliable methods usually have the strength of efficiency and better performance in solving large-scale problems.

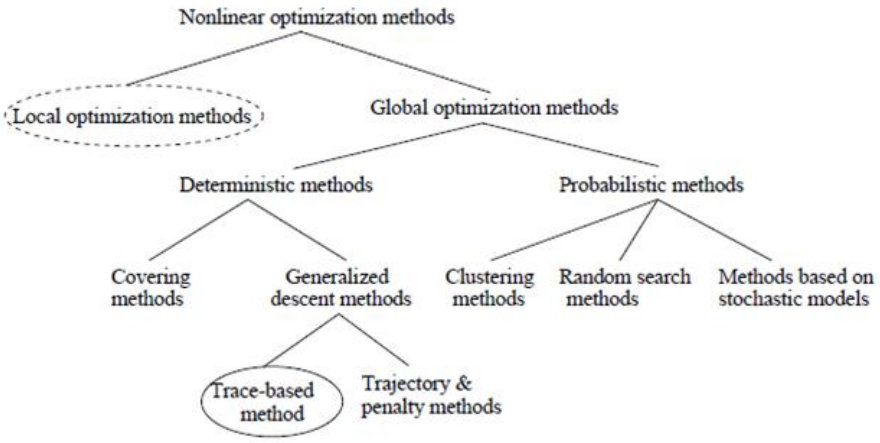

Figure 5. Classification of unconstrained nonlinear continuous global minimization methods.

3.2 Evidence for the sub-movement theory

The idea that motor control is accomplished by combining primitive elements is not at all new but the full extent of its ramifications for motor control may not yet have been fully articulated. In fact, although the experimental observations suggest that sub-movements are ubiquitous, proof of their existence and detailed quantification of their form have been elusive.

The latter is important because if the sub-movement shape was known (e.g., the time profile of any measured variable such as velocity), then decomposition to extract sub-movements from a continuous-movement record would be feasible; without it, the problem is indeterminate (a classical example of a hard inverse problem) as any compactly supported function f(x) can be approximated with arbitrary precision in the L2-sense (mean-squared convergence) by a weighted sum of ridge functions or radial basis functions [Cybenko, 1989; Hornik et al, 1989; Poggio et al, 1990].

Thus, any of an infinite set of candidate sub-movement shapes could fit with little objective basis to choose between them. One way to resolve this problem would be to observe the shape of a sub-movement in isolation. A unique opportunity to do so arose from our ongoing work studying the feasibility of applying robotic technology to assist neurological recovery.

Kinematic records of the arm movements of patients recovering from a focal brain injury (stroke) showed compelling evidence for the first time that early post-stroke recovered motions are composed of isolated segments; and that these segments become progressively more blended or overlapped as recovery proceeds.

From the above-mentioned studies, the common factor which can be observed in the composition of sub-movements is that the velocity profiles of the primary movement and those of both corrective or overlapping sub-movements seem to be characterized by constant behaviors in terms of duration, shape, mutual overlapping and a properly optimized scaling of amplitude and number.

All these available evidence point toward sub-movements' existence and no other theory has been proposed that can account for observations of movement segmentation *but* there is no obvious way to prove their existence.

In fact, the nervous central system controls the behavior of complex kinematically redundant biomechanical systems *but* how it exactly computes appropriate commands to generate movements is unknown. Particularly each individual realization of a motor goal results from the choice of one among an infinite number of motor patterns [Bernstein, 1967]. On the other hand, even if a movement can be decomposed into discrete units, that does not necessarily imply that it is was created by summing discrete units. Finally, there is no univocal relationship between motor goals and motor patterns, a property first noted to be central to the functioning of motor systems by [Lashley, 1933], which he called *motor equivalence*. Hence, the important disadvantages of the composability theory of the movement is the concomitant difficulty of identifying sub-movements unambiguously from a continuous motion record, since the sub-movements represent only one of the some ways to describe the infinite patterns that can describe the reality motor.

Moreover, it is very difficult to determinate whether what appear to be continuous adjustments of the primary movement are prearranged planned in this way by the SNC, or if these adjustments are organized according to the visual and proprioceptive feedback acquired during the execution of a motor task.

However, a strong contribute to the composability theory of the human movement has been reported recently by Hogan [Hogan et al, 2012] in which is proposed a framework for how humans physically interact with and manipulate objects. He stated that despite the *slowness* of the neurons and muscles of the human neuromuscular system, humans achieve astonishing dexterity manipulating objects—and especially using tools—far superior to anything yet achieved in robotic systems. This behavior is allowed encoding the movement solely in terms of these primitive dynamic actions, so dramatically simplifying the control of physical interaction with complex dynamic objects and the generation of complex movement.

3.3 The importance of a good initial guess in the decomposition models

Consequence of the foregoing statement, sub-movement decomposition is a non-linear optimization problem: simultaneously maximizing goodness of fit and minimizing the number of sub-movements used, given a sub-movement shape, e.g. minimum-jerk or Gaussian and a summing modality, e.g. scalar summation, or vector summation.

Many such models [Hogan, 1984; Crossman et al, 1983; Morasso et al, 1982; Flash et al, 1991] have described mechanisms and control structures that may underlie the specific motor behavior to compose a movement. These models have employed different mathematical tools, ranging from Bayesian statistics to nonlinear dynamics and optimal feedback control, to name just a few.

While useful, insights gained thereby have proven difficult to integrate with other models (which are often seen as competing theories) and more or less impossible to generalize.

So, given a measured virtual trajectory, there remains the challenge of identifying underlying motion primitives. However, since the posited underlying discrete commands are not directly available, there is no way to verify that a given decomposition is accurate.

"As a non-linear optimization problem, the sub-movement problem may have multiple local minima"

However, several optimization methods applied to overcome this problem are sensitive to getting caught in local minima and cannot guarantee a globally optimal solution.

One common approach to identifying sub-movements is to examine derivatives of the trajectory to identify local peaks, but that method is completely unreliable. Particularly, a composite of two smooth sub-movements may yield one, two, or three local velocity peaks.

Any method that uses the number of peaks to estimate the number of sub-movements would fail to make an initial guess in the neighborhood of the global optimum. Listed below are several methods for making initial guesses that have been previously applied to sub-movement decomposition. The first two methods are based on a subjective selection [Lee et al, 1997] and on identifying of local peaks [Milner et al, 1990].

Lee has made initial guesses based on subjective estimation of sub-movement characteristics. All the parameters of individual sub-movements are adjusted by hand to provide a reasonable fit to the data before to search algorithm was initiated. This method is subject to the limitations illustrated in Figure 3; sub-movement characteristics are difficult to intuit based on the speed profile, and therefore the initial guess is not guaranteed to be near the global optimum.

Milner, instead, used zero velocity and maximum curvature points along individual axes to mark the onset of sub-movements in 3D movements. Particularly, the onset of each sub-movement was determined by comparing corresponding points on the hand path and the velocity trajectory. Sub-movement onsets were so chosen to correspond to abrupt changes in hand path direction that corresponded to zero crossings or inflections in the velocity.

As implemented, Milner's method is dependent on the choice of coordinate system and leads to a somewhat arbitrary division of the movement into sub-movements. Using maximum curvature points as sub-movement delimiters suffers additionally from the fact that, although curvature tends to be maximum between sub-movements, it still does not need to be significant. Consecutive sub-movements in the same direction may have no clear peak in curvature by which to distinguish them.

Alternative methods use “greedy” algorithms which first find a sub-movement that best fits the trajectory in some suitable sense (least residual error, highest peaks peed, etc.), then subtract it and repeat the procedure on the residual until the error between the sum of sub-movements and the original trajectory falls below a specified threshold. Unfortunately, these methods also yields spurious decompositions (Figure3). Even in a simulated “test” case, where a sequence of sub-movements is known a-priori and used to compose a continuous trajectory, these methods cannot reliably recover the underlying sub-movements. Particularly, are now reported the most famous greedy algorithm used in this context.

The *Matching Pursuit* is a “greedy” algorithm; it finds the best fit for a single element at a time, rather than for a set of elements. Matching Pursuit iteratively finds the sub-movement which, when subtracted from the function, minimizes the residual error. This repeats until some minimum error threshold is reached. The limitations of the Matching Pursuit algorithm are described in detail by Chen et al. [Chen et al, 1998].

The fact that Matching Pursuit fits a single sub-movement at a time does not allow it to optimize the fit for all sub-movements. Simple functions composed of as few as two sub-movements are incorrectly decomposed, because of the greedy nature of the algorithm, as shown by Doeringer [Doeringer, 1999].

The *Irregular Sampling Radial Basis Function algorithm* [Krebs, 1997] and the *method of Berthier* [Berthier, 1996] are also greedy algorithms. At each iteration, both of these algorithms fit a sub-movement to the highest speed peak and its local neighborhood, and the fit function is subtracted from the original speed profile. As in Matching Pursuit, the process is repeated until either an error threshold is reached or a maximum number of sub-movements are fit. As illustrated in Figure 3, aligning sub-movements with the highest speed peak provides no guarantee that the sub-functions chosen

actually coincide with those used to construct the original function.Another greedy algorithm, *High Resolution Pursuit* (HRP) [Jaggi et al, 1997] is similar to Matching Pursuit in that it minimizes the residual error, but differs in that it emphasizes local fidelity of the fit and does not necessarily seek out the highest peak. Unfortunately, local fidelity of fit is not generally the best way to estimate sub-movements' characteristics. Consider for example the movement depicted in Figure 9; HRP would likely fail to make an accurate initial guess for a speed profile, since the chief characteristics of the speed profile do not resemble any of its component sub-movements.

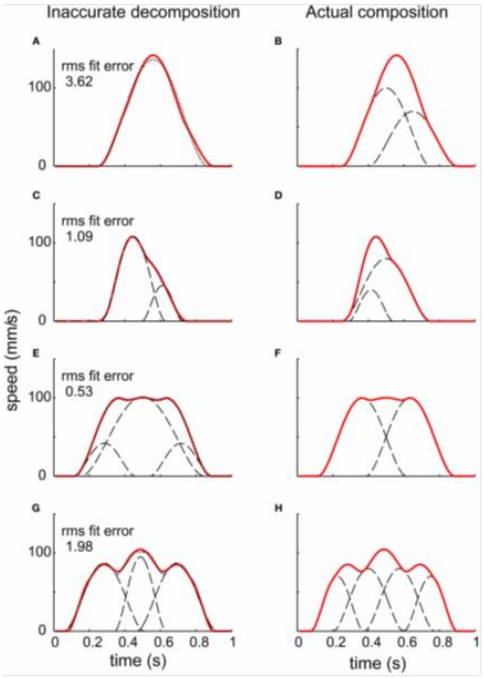

Figure 6. The challenge of decomposing a continuous trajectory into sub-movements [Rohrer et al, 2003]. The right column shows simulated speed profiles resulting from different combinations of underlying sub-movements. Note that the number of peaks does not correspond to the number of sub-movements. The left column shows the result of decomposition using "greedy" algorithms. Though the RMS fitting error is low, the sub-movements identified do not resemble those used to construct the speed profiles.

The optimality of the solution for these methods depends heavily on the quality of the initial guess; unless the initial guess is in the neighborhood of the global minimum, they will not find the best solution. In order to reliably find the global minimum and solve the decomposition problem accurately, an algorithm capable of global nonlinear optimization is necessary.

To this scope, the *Branch-and-Bound* global optimization method has been developed which avoid spurious decompositions.

The idea underlying branch-and-bound algorithms is simple: to find the global minimum of a function over a bounded parameter space, repeatedly divide (branch) the parameter space into subspaces and bound the value of the function over each subspace. If the lower bound of the function over a subspace is higher than a known value of the function elsewhere, that subspace need not be searched further. This continues until the location of the solution is known sufficiently well. This algorithm requires that each parameter be bounded. The application of the branch-and-bound algorithm to sub-movement extraction is straightforward. Consider a speed profile, g, and the current estimate of the speed profile f(p), given by

$$f(p) = \sum_{j=1}^{N} \lambda_j$$

where each λj is a sub-movement, completely described by m parameters. p is a vector containing the parameters of all the sub-movements. If N is the total number of sub-movements, then the total number of parameters in p, is given by M = N ∗m.

The formulation in the above equation assumes scalar summation of sub-movements, but could be generalized to other modes of combination. The objective function to be minimized is the absolute error, ε. With this method it has been shown that (1) the statistics of the extracted sub-movement parameters are robust to the assumed

sub-movement shape and (2) the errors introduced by inappropriate sub-movement shapes can be detected even in the presence of substantial measurement noise (Rohrer et al,2003,2006).

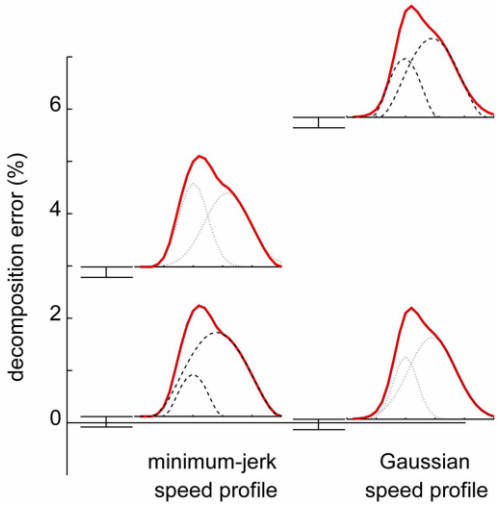

Figure 7. Ability of decomposition based on global optimization to discriminate different sub-movement shapes underlying a speed profile (Rohrer et al, 2003). Solid lines: simulated speed profiles. Dotted lines: Gaussian sub-movements. Dashed lines: minimum-jerk sub-movements.

However, although this approach, compared to the previous "*local methods*", more accurately describes the kinematic signatures of sub-movements, reduces the description error to near zero and provides a more plausible biological account of the phenomenon, it introduces a new problem for decomposition. Due to the computational demands of that approach, has been developed an alternative sub-movement extraction algorithm based on the notion of "scattershot" optimization, which is local optimization starting from a number of random initial conditions. The scattershot algorithm finds the globally optimal sub-movement composition probabilistically, i.e., the probability of finding the globally best fit can be made arbitrarily close to 1 by increasing the number of *random* starting points used in the optimization.

Chapter 4

A robust EM algorithm for the sub-movements extraction

In this chapter, we will introduce the basics about mixture models. Then, we introduce mixture models formally, show how a mixture model can be efficiently estimated with the expectation-maximization (EM) algorithm. Then we discuss the critical aspects of the EM algorithm such as the parameters initialization and determination of the number of components composing a finite mixture. These issues are particularly felt in the sub-movements theory where the shape and the number of building blocks composing a motor task is not known. Finally we illustrate and apply a robust EM algorithm to decompose point-to-point reaching movements overcoming the limitations of the local approach of a simple EM.

4.1 Finite mixture models

A finite mixture model is a convex combination of two or more probability density functions. By combining the properties of the individual probability density functions, mixture models are capable of approximating any arbitrary distribution. Consequently, finite mixture models are a powerful and flexible tool for modeling complex data. Mixture models have been used in many applications in statistical analysis and machine learning such as modeling, clustering, classification and latent class and survival analysis.

4.1.1 Basics

A continuous *L*-dimensional random variable will be denoted as X = (X_1, ..., X_l , ..., X_L), where X_l corresponds to the *l*th variable. Lower case letters will be used for a particular observation (or realization) x = (x_1, ..., x_l , ..., x_L) of a variable X.

Bold face letters, such as X, will denote a data of N observations of variable X or, equivalently, a N × L matrix, where x_{il} is the value of the *i*th observation for the *l*th variable in X.

A *probability density function* (pdf) p(x) is any function defining the probability density of a variable X such that p(x) ≥ 0 and $\int_{-\infty}^{+\infty} p(x)\,dx = 1$. By integrating p(x) over an interval, we obtain the probability that variable X assumes values in the interval [a, b], that is

$$P[a \leq X_i \leq b] = \int_a^b p(x)\,dx$$

For a given pdf p(x), the expectation of X is defined as,

$$E[X] = \int_a^b xp(x)\,dx$$

In relation to the model parameters, we use the "hat" symbol to indicate an estimator. For example $\hat{\theta}$ is the estimator of parameter θ.

4.1.2 Mixture estimation models

Let X = (X_1, ..., X_j , ..., X_L) be a L-dimensional continuous random variable and x = (x_1, ..., x_L) be an observation of X. A probability density function (pdf) of a mixture model is defined by a convex combination of K component pdfs,

$$P(X/\Theta)=\sum_{k=1}^{K} a_k p_k(x/\Theta_k)$$

where $p_k(x/\Theta_k)$ is the pdf of the *k*th component, α_k are the mixing proportions (or component priors) and $\Theta = (\alpha_1, ..., \alpha_K, \theta_1, ..., \theta_K)$ is the set of parameters. We assume that

$$\alpha_k \geq 0, \text{ for } k \in \{1, ..., K\}, \text{ and}$$

$$\sum_{k=1}^{K} a_k = 1$$

By the property of convexity, given that each $p_k(x/\Theta_k)$ defines a probability density function, $p(x|\Theta)$ will also be a probability density function. The most straightforward interpretation of mixture models is that the random variable X is generated from K distinct random processes. Each of these processes is modeled by the density $p_k(x/\Theta_k)$, and α_k represents the proportion of observations from this particular process. For example, the mixture in Figure 11 (a) models a bimodal density generated by two independent processes. A mixture can also, by combining simpler densities, model pdfs of arbitrary shapes. For example, with two Gaussian densities as components, we can model a skewed density Figure 11 (b), or a heavy tail density Figure 11 (c).

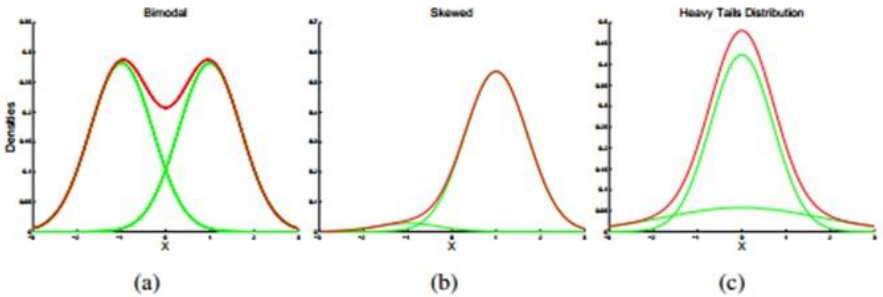

Figure 8. Examples of densities modeled by mixtures of two Gaussians pdfs. Green lines indicate the individual component densities and red lines the mixture densities. In Figure (a), we have a highly overlapping bimodal density, while in Figure (b), we depict an unimodal density skewed to the left, while in Figure (c) a density with

heavy tails. These are only a few examples representing the power of mixture models in modeling densities of arbitrary shapes.

For a given data X with N observations, the likelihood of the data assuming that x*i* are independently distributed is given by

$$p(X/\Theta)= L(\Theta/X) = \prod_{i=1}^{N} \sum_{k=1}^{K} a_k p_k(x_i/\Theta_k). \quad \text{(a)}$$

The problem of mixture estimation from data X can be formulated as to find the set of parameters Θ that gives the *maximum likelihood estimate (MLE)* solution

$$\Theta^* = \arg\max_{\Theta} L(\Theta|X).$$

The summation inside the product in (a) prevents the possibility of analytical solutions. One alternative is to maximize the complete likelihood in an expectation-maximization (EM) approach.

4.1.3 The Expectation Maximization (EM) for the Gaussian mixtures

A representation theorem of Lebesgue ensures that each random variable is represented as a mixture of distributions continuous and/or discrete and/or singular.

For $\underline{x} \in R^d$ we can define a Gaussian mixture model by making each of the K components a Gaussian density with parameters $\underline{\mu}_k$ and Σ_k. Each component is a multivariate Gaussian density

$$p_k(x|\theta_k) = \frac{1}{(2\pi)^{d/2}|\Sigma k|^{1/2}} e^{-1/2(\underline{x}-\underline{\mu k})^t \Sigma_k^{-1}(\underline{x}-\underline{\mu k})}$$

with its own parameters $\theta_k = \{\underline{\mu}_k , \Sigma_k\}$.

The EM algorithm is a very general iterative clustering algorithm for parameter estimation by maximum likelihood when some of the

random variables involved are not observed i.e., considered missing or incomplete.

The EM algorithm formalizes an intuitive idea for obtaining parameter estimates when some of the data are missing:

i. replace missing values by estimated values,

ii. estimate parameters.

iii. Repeat

- step (i) using estimated parameter values as true values, and
- step (ii) using estimated values as "observed" values, iterating until convergence.

This idea has been in use for many years before Orchard and Woodbury (1972) in their missing information principle provided the theoretical foundation of the underlying idea. The term EM was introduced in Dempster, Laird, and Rubin (1977) where proof of general results about the behavior of the algorithm was first given as well as a large number of applications. Suppose that we have a random vector $\boldsymbol{y}$ whose joint density $f(\boldsymbol{y}; \boldsymbol{\theta})$ is indexed by a p-dimensional parameter $\boldsymbol{\theta} \in \Theta \subseteq R^p$.

If the *complete-data* vector y were observed, it is of interest to compute the *maximum likelihood estimate* of $\boldsymbol{\theta}$ based on the distribution of $\boldsymbol{y}$.
The log-likelihood function of $\boldsymbol{y}$

$$\log L(\boldsymbol{\theta}; \boldsymbol{y}) = l(\boldsymbol{\theta}; \boldsymbol{y}) = \log f(\boldsymbol{y}; \boldsymbol{\theta}),$$

is then required to be maximized.

In the presence of missing data, however, only a function of the *complete-data* vector $\boldsymbol{y}$, is observed. We will denote this by expressing $\boldsymbol{y}$ as ($\boldsymbol{yobs}$, $\boldsymbol{ymis}$), where $\boldsymbol{yobs}$ denotes the observed but "incomplete" data and $\boldsymbol{ymis}$ denotes the unobserved or "missing" data.

For simplicity of description, assume that the missing data are missing at random (Rubin, 1976), so that

$$\begin{aligned} f(\boldsymbol{y}; \boldsymbol{\theta}) &= f(\boldsymbol{y}_{obs}, \boldsymbol{y}_{mis}; \boldsymbol{\theta}) \\ &= f_1(\boldsymbol{y}_{obs}; \boldsymbol{\theta}) \cdot f_2(\boldsymbol{y}_{mis}|\boldsymbol{y}_{obs}; \boldsymbol{\theta}), \end{aligned}$$

where f_1 is the joint density of $\boldsymbol{y}_{obs}$ and f_2 is the joint density of $\boldsymbol{y}_{mis}$ given the observed data $\boldsymbol{y}_{obs}$, respectively. Thus it follows that

$$l_{obs}(\boldsymbol{\theta}; \boldsymbol{y}_{obs}) = l(\boldsymbol{\theta}; \boldsymbol{y}) - \log f_2(\boldsymbol{y}_{mis}|\boldsymbol{y}_{obs}; \boldsymbol{\theta}),$$

where $l_{obs}(\boldsymbol{\theta}; \boldsymbol{y}_{obs})$ is the observed-data log-likelihood.

EM algorithm is useful when maximizing l_{obs} can be difficult but maximizing the complete data log-likelihood l is simple.
However, since y is not observed, l cannot be evaluated and hence maximized. The EM algorithm attempts to maximize $l(\boldsymbol{\theta}; \boldsymbol{y})$ iteratively, by replacing it by its conditional expectation given the observed data $\boldsymbol{y}_{obs}$.

This expectation is computed with respect to the distribution of the complete-data evaluated at the current estimate of $\boldsymbol{\theta}$. More specifically, if $\boldsymbol{\theta}^{(0)}$ is an initial value for $\boldsymbol{\theta}$, then on the first iteration it is required to compute

$$Q(\boldsymbol{\theta}; \boldsymbol{\theta}^{(0)}) = E_{\theta(0)} [l(\boldsymbol{\theta}; \boldsymbol{y})|\boldsymbol{y}_{obs}].$$

$Q(\boldsymbol{\theta}; \boldsymbol{\theta}^{(0)})$ is now maximized with respect to $\boldsymbol{\theta}$, that is, $\boldsymbol{\theta}^{(1)}$ is found such that

$$Q(\boldsymbol{\theta}^{(1)}; \boldsymbol{\theta}^{(0)}) \geq Q(\boldsymbol{\theta}; \boldsymbol{\theta}^{(0)})$$

for all $\boldsymbol{\theta} \in \Theta$.

Thus the EM algorithm consists of an **E-step** (Estimation step) followed by an **M-step** (Maximization step) defined as follows:

E-step: Compute $Q(\boldsymbol{\theta}; \boldsymbol{\theta}^{(t)})$ where

$$Q(\boldsymbol{\theta}; \boldsymbol{\theta}^{(t)}) = E_{\boldsymbol{\theta}(t)}[l(\boldsymbol{\theta}; \boldsymbol{y})|\boldsymbol{y}_{obs}] .$$

M-step: Find $\boldsymbol{\theta}^{(t+1)}$ in Θ such that

$$Q(\boldsymbol{\theta}^{(t+1)}; \boldsymbol{\theta}^{(t)}) \geq Q(\boldsymbol{\theta}; \theta^{(t)})$$

$$\text{for all } \boldsymbol{\theta} \in \Theta.$$

The E-step and the M-step are repeated alternately until the difference $L(\boldsymbol{\theta}^{(t+1)}) - L(\boldsymbol{\theta}^{(t)})$ is less than δ, where δ is a prescribed small quantity.

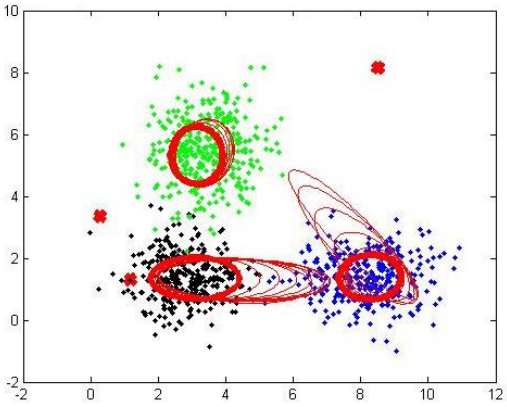

Figure 9. Example of Expectation Maximization of Gaussian Mixture Models.

The computation of these two steps simplify a great deal when it can be shown that the log-likelihood is linear in the sufficient statistic for θ. In particular, this turns out to be the case when the distribution of the complete-data vector (i.e., $\boldsymbol{y}$) belongs to the exponential family.

In this case, the E-step reduces to computing the expectation of the complete-data sufficient statistic given the observed data. When the complete-data are from the exponential family, the M-step also simplifies. The M-step involves maximizing the expected log-likelihood computed in the E-step. In the exponential family case, actually maximizing the expected log-likelihood to obtain the next iterate can be avoided. Instead, the conditional expectations of the sufficient statistics computed in the E-step can be directly substituted for the sufficient statistics that occur in the expressions obtained for the complete-data maximum likelihood estimators of θ, to obtain the next iterate.

As a general algorithm available for complex maximum likelihood computations, the EM algorithm has several appealing properties relative to other iterative algorithms such as Newton-Raphson. First, it is typically easily implemented because it relies on complete-data computations: the E-step of each iteration only involves taking expectations over complete-data conditional distributions. The M-step of each iteration only requires complete-data maximum likelihood estimation, for which simple closed form expressions are already available. Secondly, it is numerically stable: each iteration is required to increase the log-likelihood $l(\boldsymbol{\theta}; \boldsymbol{y}_{\text{obs}})$ in each iteration, and if $l(\boldsymbol{\theta}; \boldsymbol{y}_{\text{obs}})$ is bounded, the sequence $l(\boldsymbol{\theta}^{(t)}; \boldsymbol{y}_{\text{obs}})$ converges to a stationery value. If the sequence $\boldsymbol{\theta}^{(t)}$ converges, it does so to a local maximum or saddle point of $l(\boldsymbol{\theta}; \boldsymbol{y}_{\text{obs}})$ and to the unique MLE if $l(\boldsymbol{\theta}; \boldsymbol{y}_{\text{obs}})$ is unimodal. A disadvantage of EM is that its rate of convergence can be extremely slow if a lot of data are missing: Dempster, Laird, and Rubin (1977) show that convergence is linear with rate proportional to the fraction of information about θ in $l(\boldsymbol{\theta}; \boldsymbol{y})$ that is observed.

4.1.4 Problems of the EM algorithm

Normal mixture are widely used as a modelling tool in many fields of study. A major statistical problem arising in their use is that of the estimation of the parameters. In fact, it is known that the problems arise when the method of maximum likelihood is used to estimate the parameter of a mixture of normal distributions. the most popular algorithm for computing maximum likelihood estimates in the normal mixture case is the EM algorithm, which has several good computational properties, including a low storage requirement and a low work cost per iteration. However, the EM algorithm is characterized by two critical limitations:

- ***Number of Components***

Typical implementations of Expectation Maximization require the user to specify the number of model components. This is problematic because users do not generally know the correct number of components. Choosing too many or too few components can lead to over-fitting or under-fitting, respectively (Figure 13). This problem is particularly *felt* in the decomposition problem of the reaching movements, where is not known *in advance*. The traditional approach is to choose the optimal number of components by some cost-function based criteria such as Akaike's information criterion (AIC). However, since it is needed to repeat the entire parameter estimation at a number of different M, the process of evaluating these criteria incurs in a large computational cost. Figueried & Jain [Figueried et al, 2002] annihilates the number of components from a large M to obtain optimal M*. But how to know which M we start from? Wang [Wang et al, 2004] proposed stepwise split-and-merge EM (SSMEM) algorithm to choose M and estimate parameters simultaneously.

However, the frequent operations of splitting and merging components of FMM also lead to large computational cost [Chen and Luo, 2004].

Others methods have been proposed in the literature to estimate the number of components in a mixture of Gaussians, among which MDL method, Bayesian information criterion and Akaike's information criterion. These estimators are motivated from different theories that translate, in practice, to different penalty factors in the formulation used to select the best model. The MDL criterion is based upon an information-theoretic view of induction as data compression. It is equivalent to the Bayesian information criterion, which gives a Bayesian interpretation.

Akaike's information criterion is a statistical hypothesis test derived from a different theoretical perspective: it is an optimal selection rule in terms of prediction error; that is, the criterion identifies a finite-dimensional model that, while approximating the data provided, has good prediction properties. The decision of which criterion is more meaningful is entirely a matter of interpretation, and depends on the specific application).

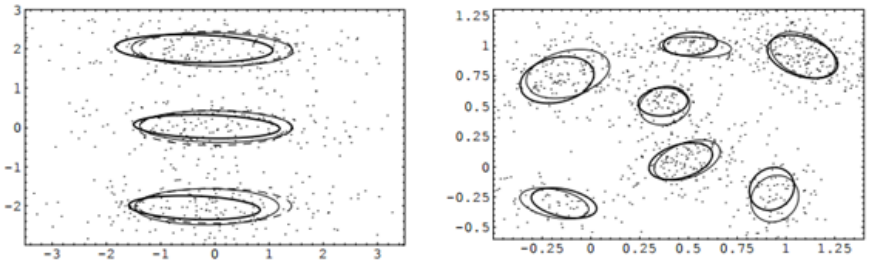

Figure 10. Results of EM mixture estimation initialized by two and seven components.

- ***Parameter Initialization***

Choosing appropriate initial parameter values can have a significant effect on the quality of the solution. it is widely acknowledged that EM suffers from some issues. Firstly, it is highly sensitive to initialization, being a local maximum seeker; secondly, when the likelihood function is unbounded (for instance in the case of heteroscedastic model) the algorithm may converge to some singularities and this causes the failure of the optimization procedure.
So, EM is not guaranteed to converge to the global maximum of the likelihood function but may instead converge to a local maximum. Therefore different initial parameter values can lead to different model parameters and different model quality. A variety of ways to find better local optima have been explored, including heuristic initialization of the model parameters (Spitkovsly et al, 2010) random restarts (Smith, 2006), and annealing (Smith and Eisner, 2006; Smith, 2006).

4.2 A robust EM method

In the context of the likelihood approach to mixture modeling, many authors used the expectation-maximization (EM) algorithm for estimating the parameters of the model. However, it is widely acknowledged that EM, in this framework, suffers from some issues. Firstly, it is highly sensitive to initialization, being a local maximum seeker; secondly, when the likelihood function is unbounded (for instance in the case of heteroscedastic model) the algorithm may converge to some singularities and this causes the failure of the optimization procedure. These phenomena have been well studied for normal mixtures and under suitable conditions, constrained global maximum likelihood formulations have been proposed, which present no singularities and a smaller number of spurious maxima. However, these issues may still be observed in mixtures of t distributions. Thus,

in order to prevent or reduce such drawbacks, a constrained EM algorithm for mixture distributions is now proposed. The algorithm used here, defined as a constrained EM by Chen (Chen et al, 1992), is altered using simple constraints which increase robustness against poor initial guesses while maintaining a low work requirement per iteration. The modified algorithm is described and is applied to the decomposition problem of the human reaching movements.

4.2.1 A new sub-movement model

The velocity profiles of the upper limb reaching movements are modelled in order to extract sub-movements composing subject overall motion taking cue on the well-known minimum jerk theory which states that the shape of the velocity profile of the hand, in point-to-point human arm movements restricted to a horizontal plane, is bell-shaped and symmetrical. So, the velocity profiles are modeled as the summation of Gaussian pulses of various lengths (Chen et al, 1992) in mathematical terms according to the expression:

$$\text{b)}\quad y(\mathrm{x}) = \sum_{i=1}^{M} \frac{\alpha_i}{\sqrt{2\pi\sigma_i^2}} \exp\left[- \frac{(\mathrm{x} - \mu_i)^2}{2\sigma_i^2} \right]$$

where $\boldsymbol{\alpha_i}$ is the amplitude of the basic function, $\boldsymbol{\mu_i}$ and $\boldsymbol{\sigma_i}$ are respectively the mean and standard deviation of the Gaussian base functions, M is the number of pulses and a constrained-Expectation–Maximization (CEM) algorithm is used for the mixture parameters by first computing an estimate of the parameter and then refining the estimate by maximizing a likelihood function (maximum-likelihood estimation method, MLE).

Essentially, MLE involves estimating the parameters by maximizing the likelihood function, $l(X;\Theta)$, this being simply the joint probability of the observations x_j regarded as a function of the parameters:

$$l(X;\Theta) = \prod_{j=1}^{N} f(x_j;\Phi)$$

where N is the number of observation points and $f(x_j; \Phi)$ is a mixture of M normal density functions as

$$f(x_j;\Theta) = \sum_{i=1}^{M} a_i f_i(x_j;\ \mu_i;\sigma_i)$$

The EM algorithm iteratively generates, starting from some initial approximation $\Phi^{(0)}$, a sequence $\Phi^{(r)}$ of estimates.

Each iteration consists of the following two steps.

E-Step: Estimate the belonging of each observation x_j to the Gaussian components $w_i = f_i(x_j;\ \mu_i,\ \sigma_i)$ by calculating the *a posteriori* probabilities according to

$$\hat{p}^{(r)}(w_i\ x_i) = \frac{\alpha_i^{(r)} f(x_j;\ \mu_i^{(r)},\ \sigma_i^{(r)})}{\sum_{i=1}^{M} \alpha_i^{(r)} f(x_j;\ \mu_i,\ \sigma_i)}, \qquad j = 1, \cdots, N.$$

where w_i is the Gaussian probability density function of the i-th component

$$w_i(x, \mu, \sigma) = \frac{1}{\sqrt{2\pi\sigma_i^2}} exp^{[-\frac{(x-\mu_i)^2}{2\sigma_i^2}]}$$

M-Step: Find $\Phi = \Phi(r + 1)$ to maximize the likelihood function according to

$$\alpha_i^{(r+1)} = \frac{1}{N}\sum_{j=1}^{N} \hat{p}^{(r)}(w_i\, x_j) f(x_j;\, \phi^{(r)})$$

$$\mu_i^{(r+1)} = \frac{\sum_{j=1}^{N} \hat{p}^{(r)}(w_i\, x_j) f(x_j;\, \phi^{(r)}) x_j}{\sum_{j=1}^{N} \hat{p}^{(r)}(w_i\, x_j) f(x_j;\, \phi^{(r)})}$$

$$\sigma_i^{2(r+1)} = \frac{\sum_{j=1}^{N} \hat{p}^{(r)}(w_i\, x_j) f(x_j;\, \phi^{(r)}) (x_j - \mu_i^{(r+1)})^2}{\sum_{j=1}^{N} \hat{p}^{(r)}(w_i\, x_j) f(x_j;\, \phi^{(r)})}.$$

4.2.2 Constrained optimization

Usually the M-step is an unconstrained maximization but here the EM algorithm is altered using simple constraints which increase robustness against poor initial guesses. Particularly, here the M-step is performed on the set $\Omega_{\varepsilon,\, c}$ given by

$$\Omega_{\varepsilon,\, c} = \{\Phi \in \Omega \,/\, \alpha_i \geq \varepsilon,\ \sigma_i \geq c * \sigma_{i+1} \qquad \forall i = 1, \ldots \ldots \ldots M\}$$

where ε=0.01 and c=0.2 are the constrains introduced on the α and on the σ of each component, respectively, while the set Ω

Ω=

$$\{\Phi = (\alpha_1, \ldots\ \alpha_M, \mu_1, \ldots \mu_M, \sigma_1, \ldots \sigma_M / \sum \alpha_i, \alpha_i \geq 0, \sigma_i \geq 0) \qquad \forall i = 1, \ldots \ldots \ldots M\}$$

is the set of solutions whiteout the constrains introduced by the CEM algorithm.

Summarizing, the two steps of the CEM algorithm are:

- Definition of the current maximization model $M^r(\Phi)$ by means of the following equation:

$$M^r(\Phi) = \sum_{i=1}^{M}\sum_{k=1}^{N} w_i(x_k)^r \log \alpha_i + \sum_{i=i}^{M}\sum_{k=1}^{N} w_i(x_k)^r \log[f(x_k;\mu_i;\sigma_i)]$$

Computation of $\Phi\ (r+1)=\max M^r(\Phi)/\ \Phi \in \Omega_{\varepsilon,\ c.}$

4.2.3 A new approach for the initial guess

For estimating the initial set of parameters of the Gaussian functions, the goal is to find boundaries of the individual components from which the initial estimates $\mathbf{\Phi}^{(0)}$ of these parameters can be determined. The above CEM algorithm uses the scale-space filtering approach (Babaud, et al, 1986) for detecting the boundaries of one-dimensional (l-D) signals and for estimating the initial set of mixture parameters in following several steps.

At first, a Gaussian filter of standard deviation $\boldsymbol{\sigma_f}$ it is applied to smooth the input velocity profile (VP) signal by convolution, obtaining the *image-signal velocity* (*ISV*). There are several important scale-space concepts that apply to 1-D (or 2-D) signals. It has been shown (Babaud, et al, 1986; Florack et al, 1984. Witkin, 1983; Yuille and Poggio, 1986) that the scale space of almost all signals filtered by a Gaussian kernel determines the signal uniquely up to a scaling constant. The importance of this property lies in the fact that, theoretically, for almost all signals, no information is lost by working in the space scale.

Moreover has been shown that the Gaussian kernel does not create additional zero crossings as the scale $\boldsymbol{\sigma_f}$ increases beyond a certain limit and that it is the only filter with this nice scaling behavior [Yuille and Poggio, 1986].

In the second step, are recorded the pairs (upper and lower) of *turning points* which are determined from the zero-crossings of the second derivative in the ISV. Each pair of turning points are used to define the boundaries of each individual component of the mixture.
Subsequently, these two steps are repeated through the range of scales properly chosen. This is due to the fact that by applying different scales of Gaussian filtering on one signal, varied numbers of turning points can be found from the filtered signals and this means that can change the number of components in the Gaussian mixture.
The plot of the turning-point location of the filtered signal versus the scale σ_f of Gaussian filters applied is called the *fingerprint*.

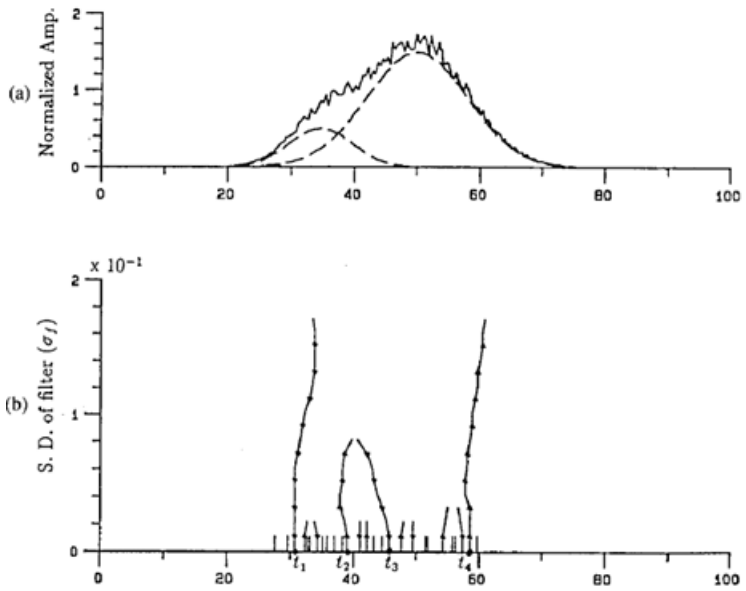

Figure 11. The fingerprint diagram (b) of a simulated signal which is a summation of two Gaussian pulses (a). In the fingerprint diagram the y-axis is the standard deviation of the Gaussian filters σ_f and the x-axis is the position of turning points in terms of percent of time duration of the Gaussian mixture.

For the Gaussian filter scale chosen, the number of initial components (M) composing the mixture is determined on the fingerprint by the number of pairs of turning points for the selected $\boldsymbol{\sigma_f}$.

Once determined the number M of components, the initial set of mixture parameters $\mathbf{\Phi}^{(0)}$ can be performed. Particularly,

- The amplitude $\boldsymbol{\alpha}_i^{(0)}$ is the proportion of area covered by the mixture relative to the overall area of the mixture.
- The mean $\boldsymbol{\mu}_i^{(0)}$ of the mixture is the midpoint of the upper and lower turning points.
- The standard deviation $\boldsymbol{\sigma}_i^{(0)}$ is half of the width between the upper and lower turning points.

The important advantage of the scale-space approach is that it provides an initial parameter estimation for the number of components, which is difficult to estimate using statistical estimation in a noisy environment. This algorithm (scale space approach followed by CEM algorithm, without) has been successfully applied to model the linear envelope of the EMG but here was repeated with appropriate adjustments. In fact, besides the *initialization of the parameters*, an important difficulty with the mixture model is the choosing the *number of components* that best suits the number of clusters (or density categories) present in the image.To find the correct number of components in a mixture is an important but very difficult problem because no reliable *a priori* information is not always available about the number of density categories in a given velocity profile of a reaching movement. Moreover, the appropriate solution depends on the amplitude of the noise which corrupt the signal. *So, the results of the algorithm depend mainly on the initial guess of the number of components of the mixture model and may converge to a spurious maximum and thus multiple solutions are always present.*
It is not clear how the CEM proposed by Chen come to the initial guess of the optimal number of components composing the mixture: particularly how to choose the optimal value of standard deviation $\boldsymbol{\sigma}_f$ of Gaussian filter (which allow to define the initial number M of components by means the fingerprint). In our application is proposed

the *discrete gradient method*, which finds the gradient vector a the scalar function f with respect to vector, for the initial guess of the number of components. In fact, frequently there is no good basis for choosing the scale $\boldsymbol{\sigma_f}$ of measurement of measurement *in advance*. It may often be desirable to describe the same signal at more than one scale in the course of interpreting it. Particularly, the Matlab gradient function is applied to the VL to find the pairs of zero-crossings of the second derivative which represent our *initial guess* K of the M-number of components composing the Gaussian model. Then the Gaussian filter scale $\boldsymbol{\sigma_f}$ is increased until the number M of components of the mixture, defined by means the relative fingerprint, is equal to the initial guess K. then, these M number can be adjusted by the CEM algorithm. Once estimated the M and the mixture parameters $\boldsymbol{\Phi}^{(0)}$, all these information enter in the CEM algorithm and are adjusted. Particularly the M of components defined by means of the discrete gradient method and by means of the scale space approach can be uploaded (reduced) considering the constrained defined in section 5.2.2. Following are showed the computing methodology for the scale-space approach, EM iteration, and constraints of the algorithm (Figure 15).

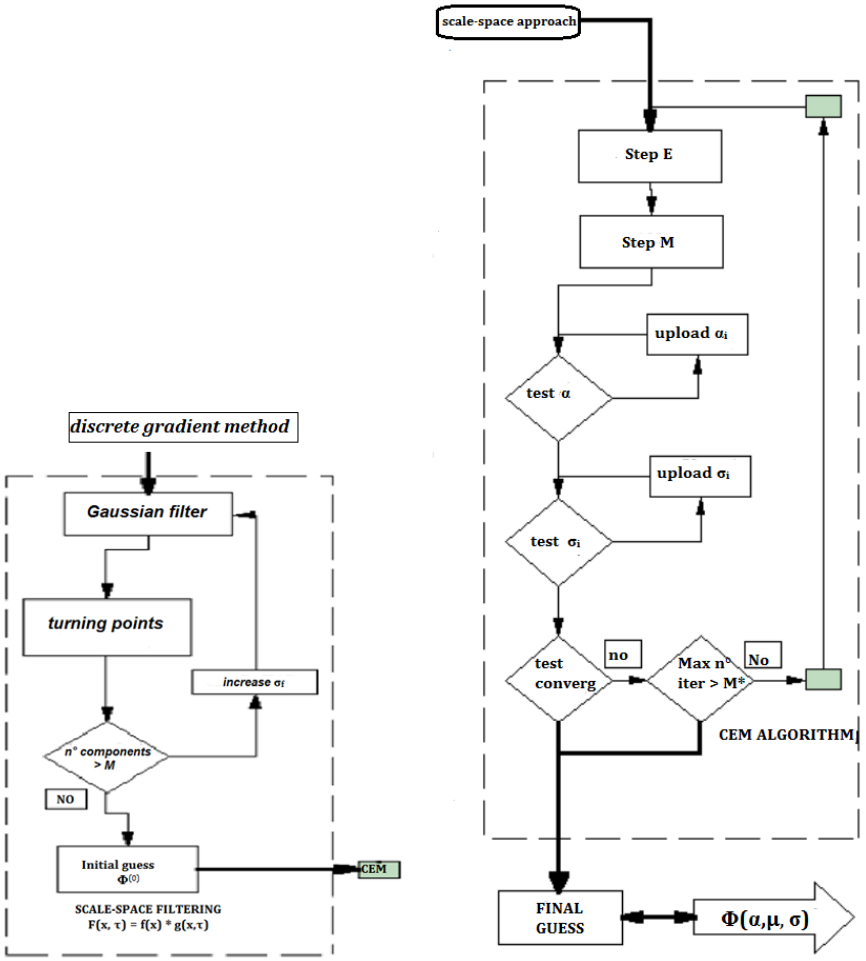

Figure 12. The space-scale approach and the CEM algorithm for the initial guess of the Gaussian functions parameters.

4.2.4 Algorithm Performance

The CEM algorithm evolves repeating E-steps and M-steps until convergence is reached according to the following equation:

$$\text{Max}\{|\alpha i(s+1)- \alpha i(s)|/ \alpha i(s); |\mu i(s+1)- \mu i(s)|/ \mu i(s); |\sigma i(s+1)- \sigma i(s)|/ \sigma i(s) \ \forall i=1 \ldots M\}$$

where s+1 is the current iteration while s is the previous iteration of the algorithm.
The convergence is reached when the above amount is less than 0.00001 or when the maximum number of iteration M* (see Figure 15) is reached.
In order to test the solution-finding performance of the above discussed algorithm, four simulated velocity profiles (Figure 16 a)-d)) have been created (gmidstribution – Statistic Toolbox –Matlab R2014a), each consisting of two Gaussian sub-movements (blue and green shapes) which characteristics which are known beforehand.

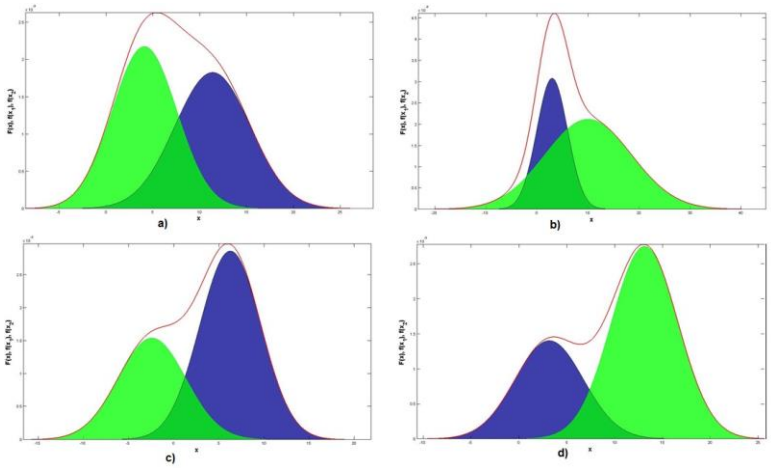

Figure 16. Four simulated velocity profiles composed of two known Gaussian sub-movements (represented with blue and green filled area).

These profiles have been decomposed (Figure 17) by means of our algorithm and the performance of the proposed method has been evaluated in the sense of root mean square error (RMSE), which was computed as. The lower values of the RMSE, ranging between the 2% and 5%, indicate a good performance of our method.

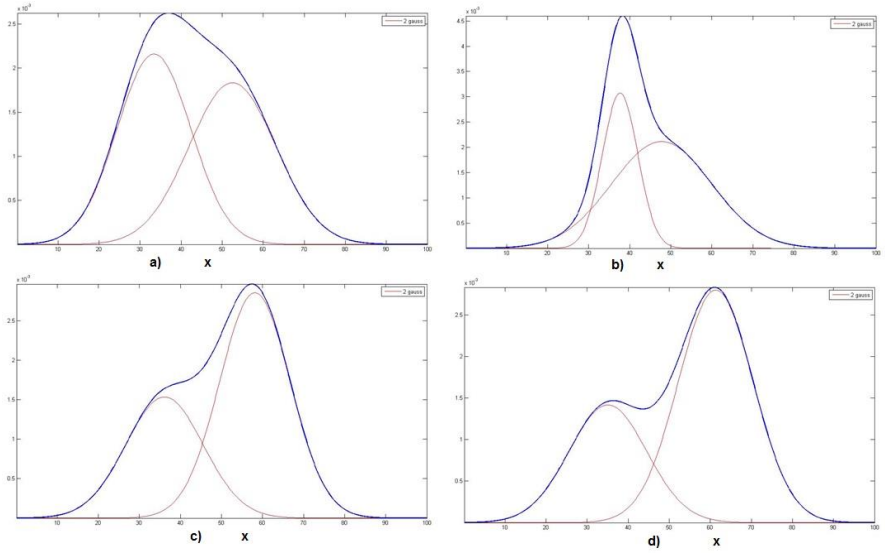

Figure 17. Decomposition of the simulated mixture normal density by means of the robust-EM.

Chapter 5

A novel approach to evaluate the arm muscle force

Reaching movements (RM) are produced by transforming parameters of the desired movement (e.g., direction, distance, and movement time) into appropriate patterns of activity in the muscles of the shoulder and elbow. Therefore it is important to study the upper arm muscle activity by means of indexes useful to evaluate changes in muscle activation and in force muscle. The main assumption is the relationship of the EMG signal to the force produced by a muscle but a simple equation describing this relationship has not yet been found. This is due to the several limitations of the EMG signal processing based on its linear envelope (LE). To overcome the drawbacks and the physiological variability of EMG and of its LE, so simplifying the evaluation of EMG patterns, we adapted the CEM algorithm to the description of the LE signal in order to propose a new way to evaluate the force muscle.

5.1 The muscle activity in the motor control

The upper-limb reaching movements are very important for the human daily activities, such as eating, drinking, brushing teeth, combing hair and washing face. These motor tasks are produced by transforming parameters of the desired movement (e.g., direction, distance, and movement time) into appropriate patterns of activity in the muscles of the shoulder and elbow. The basic motions of upper-limb can be categorized into eight individual motions and is activated by many

kinds of muscles. Some of them are bi-articular muscles and the others are uni-articular.
Therefore it is important to study the upper arm muscle activity by means of indexes useful to evaluate changes in muscle activation and in force muscle.

5.2 The electromyographic (EMG) signal

The activity of muscles has been the subject of many studies of bioengineers, physiologists, neurophysiologists, and clinicians for more than 100 years. Many different methods of gathering and interpreting the physiological data and information have been developed. The muscle movement in all human beings is controlled by the central nervous system. It generates the electrical pulses that travel through the motor nerves to different muscles. The neuromuscular junction is called innervation zone and is usually situated about the middle of the muscle body.

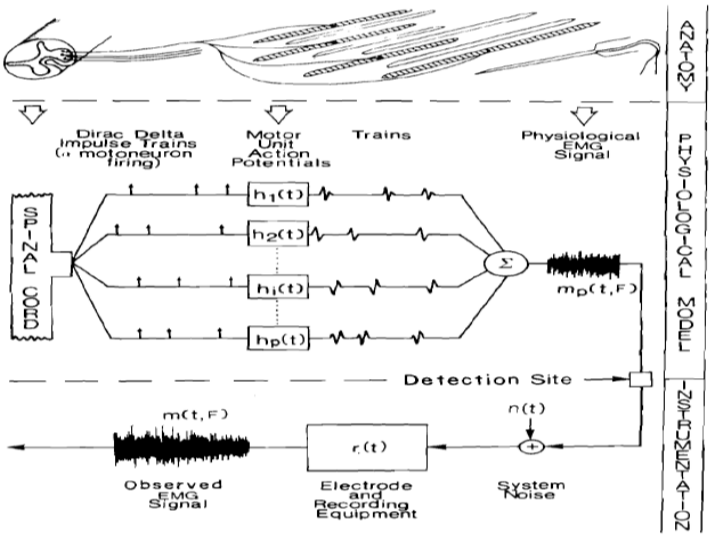

Figure 138. Schematic representation of the model for the generation of the EMG signal [Basmajian et al., 1985].

Each muscle is composed of a large number of tiny muscle fibers, which are organized into so called motor units (MU). Each MU gathers all the fibers that are innervated by the same nerve, i.e. axon. When electrically excited, fibers produce a measurable electrical potential, called action potential (AP), which propagates along the fibers to both directions towards muscle tendons and causes the contraction of the fibers. The ***electromyographic (EMG) signal*** results from the spatial and temporal summation of the electric fields generated by all muscle fibers (Figure 18).

5.3 The relation between EMG and muscle force

After recording EMG signals from a variety of muscles be further processed offline. The processing techniques applied to study muscle activation patterns depend on the type of analysis performed by the researcher and can extract different information from the raw signal. In a study analyzing muscle coordination it is common practice to extract the linear envelopes (LEs) of the recorded EMG signals.
This processing technique allows to simplify the data by eliminating some unnecessary information (such as the activation of each single motor unit, which is visible in the high frequency content), while still maintaining enough information to study muscle activation timing and amplitude. In the field of biomechanics research, the main assumption is the relationship of the EMG signal to the ***force produced by a muscle***, which is related to the amplitude of the EMG signal (Figure 19).

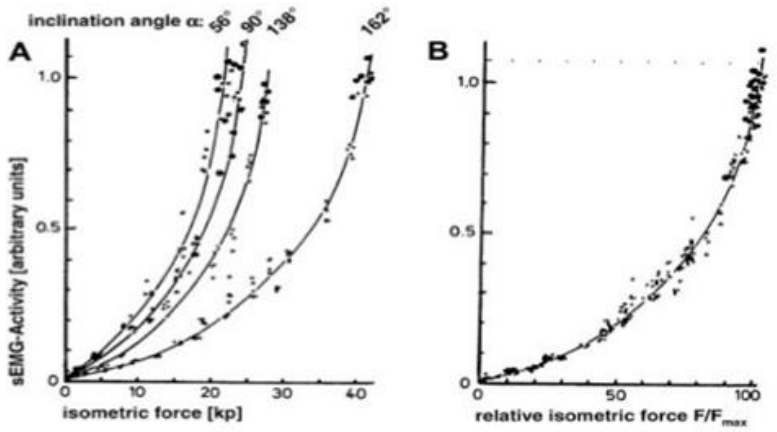

Figure19. Relationship between surface EMG and muscle force during and isometric contraction.

However, the relationship between force and surface EMG during voluntary contractions is not well understood. Some authors have concluded, for various muscles, that the magnitude of the EMG signal is directly proportional to muscle strength for isometric and/or isotonic contractions with constant speed, but others claim that this relationship is not linear (Bilodeau et al., 2003; Gregor et al., 2002; Karlsson & Gerdle, 2001). In most cases, the EMG increases non-linearly with increasing force of muscle contraction (Guimaraes et al., 1994; Madeleine et al., 2000). This variety of different interpretations among researchers not surprising, given the several *inherent limitations of surface EMG* (*or of its LE*):

- The measured force of muscle contraction is a result of the global activity of the underlying muscle fibers, and surface EMG provides information about the electrical activity of motor units located in the region near the electrode; in most experiments, *the catchment area of the electrode does not extend sufficiently to detect the signal generated across the entire muscle volume*.

- Surface EMG recordings provide a practical means to record from several muscles simultaneously but tend to be unreliable, i.e. recordings from a subject performing the same movement repetitively tend to have considerable *trial-to-trial variability*.

- Factors that prevent the direct quantification of muscle force from EMG signals include *cross-talk*, variations in the location of the recording electrodes and the involvement of synergistic muscles in force generation. The electrical cross-talk of adjacent muscles is often considered as a possible factor that complicates the determination of the relationship between EMG and force. Its influence would manifest most prominently when the measured strength of the muscle increases. The presence of cross-talk is more dominant in smaller muscles where the electrodes (especially the surface) must be placed close to the adjacent musculature. The complexity of cross-talk is also determined by the anisotropy of muscle tissue and homogeneity of the tissues adjacent to the muscle. The degree of synergistic action of other muscle groups and the amounts of co-contraction between antagonistic muscle groups can change the contribution of muscle strength in research on the net force measured in the joint. This results in a great variability of the EMG traces.

The force muscle could be assess subjectively through using, for example, the *peak of the LE* identified by using a threshold value. The main limitation of this approach is that the threshold level used for the peak identification of the LE is mainly dependent on the signal-to-noise ratio, so determining the trade-off between missed spikes (false negatives) and the number of background events that cross the threshold (false positives). Moreover, in our opinion, even if correctly identified, the peak of the LE gives information to the maximum strength developed in a very short period.

5.4 The peak Phase as an index of the muscle force

In this study to overcome all the above described drawbacks and the physiological variability of EMG and of its LE, so simplifying the evaluation of EMG patterns, we adapted the CEM algorithm to the description of the LE signal. Particularly, we suppose that the EMG envelope created by a reaching or grasping movement is a composite of phases of activity, i.e. acceleration and deceleration phases, so the mixture of Gaussian model, in which the components are pulse-like, is an appropriate mathematical model to describe such motor tasks. So, using the algorithm described in section 4 of this thesis, the linear envelopes (LEs) of several EMG signal recorded during reaching movements, are modelled as summation of Gaussian pulses of various length and amplitude. The dominant phase with the largest amplitude $\boldsymbol{\alpha_i}$ attribute is further defined as the *peak activity or peak phase (PA)* of the LE. In the following we will use the acronym PA to indicate the position of peak value of the PA over the reaching movement time duration (%). A physical significance of this dynamic index can be attributed to the temporal muscle activation and to the *phase involving a considerable underlying muscle effort* while the peak of the LE, used increasingly for the assessment of normal and pathological muscle activity, gives information to the maximum strength developed in a short period. In the next section we will better explain the procedure used to define the PA.

Chapter 6

A novel approach in rehabilitation field of upper arm

In the last few years, the RM derive their growing importance not only by the contribution they give to the understanding of the movement physiology, but also to their diffusion in rehabilitative field. Upper limb RM are in fact the most used motor task in rehabilitation treatments of several disorders of the arm and the shoulder of various central and peripheral etiology.

Despite the increasing effort put in the development of robotic systems for neuro-rehabilitation, justified by the big potential of such applications as additional end efficient tools for therapy, their clinical effectiveness is still being discussed. Many of the systems developed to date were designed from an engineering point of view and do not meet therapy demands, which is reflected by unsatisfactory clinical outcomes.

Here is proposed a quantitative kinematic and electromyographic assessment of robot assisted upper arm reaching. Particularly, we study the quality and the motor composition of visually-guided reaching movements from people with pathological conditions, such as stroke disease, applying the minimum jerk theory and the decomposition method proposed in section 4 to identify the sub-movements and to estimate the force muscle involved.

6.1 Limits of the robotic rehabilitation

Reaching movement is a movement executed towards a given target and represents a basic movement of the upper extremities, very important for independence in daily living activities such as self-feeding, grooming, dressing and environmental switch operations.
In the last few years, the RM derive their growing importance not only by the contribution they give to the understanding of the movement physiology, but also to their diffusion in rehabilitative field. Upper limb RM are in fact the most used motor task in rehabilitation treatments of several disorders of the arm and the shoulder of various central and peripheral etiology. Robotic rehabilitation systems are an efficient approach to this problem, as they are well suited to produce an intensive, task-oriented motor training as part of an integrated set of rehabilitation tools, including also simpler non-robotic solutions.
In fact, the labor intensive aspects of therapy can be done by the robotic system, while the therapist could focus on functional rehabilitation during individual training [Rosati, 2010]. Additionally, a single therapist could supervise multiple robotic rehabilitation stations and work on more than one patient at the same time. In other words, robotic systems could help automating the repetitive part of neuro-rehabilitation in a controlled manner. Besides improving therapy at the rehabilitation facility, affordable robotic devices would allow patients to continue rehabilitation at home [Harwin et al, 2006].
The rehabilitation robots developed in the last years can be classified roughly in passive systems, which act as support and stabilizer of the limb, active systems, relying on actuators to guide the patient through predefined movements, and interactive systems, which include more sophisticated control paradigms that react to the patient's actions [8]. The most commonly used paradigm is to use robotic devices for

physically supporting the patient during the execution of certain movements [Harwin et al, 2006, Krebs, 2007].

However, robotic systems offer far more possibilities than just the repetition of simple and stereotyped movement patterns. For example, they can generate a more complex, multisensory stimulation, they can provide the patient with extrinsic feedback containing information on his performance during training, or they can create a more engaging environment by using virtual reality concepts [Rosati, 2010]. Another advantage is that such devices can promote recovery by distorting reality. One example is the implementation of an error-augmenting strategy, i.e. the application of a force that pushes the patient away from the desired trajectory.

Indeed, preliminary results have shown that this approach can have positive effects on the patient's functional recovery [Harwin et al, 2006]. Moreover, robotic systems can measure and record a variety of variables during therapy, such as the patient's position, velocity and acceleration, or the amount of support provided by the system [Harwin et al, 2006, Rosati, 2010].

The recorded data can be used for online and offline processing, allowing to evaluate several indicators related to the patient's performance [Timmermans et al, 2009]. Such measured parameters could offer a substantial improvement over current evaluation techniques, as they would provide quantitative and objective data in contrast with today's most used assessments, which rely heavily on subjective judgments made by the clinician [Harwin et al, 2006]. It has been reported by various authors that the use of robotic systems in neuro-rehabilitation improves the patient's recovery and quality of life, especially when the robot-assisted therapy is administered in the sub-acute phase and when it is combined with traditional treatment [Timmermans et al, 2009].

Moreover, it has been reported by various authors that the use of robotic systems in neuro-rehabilitation improves the patient's recovery and quality of life, especially when the robot-assisted therapy is

administered in the sub-acute phase and when it is combined with traditional treatment [Timmermans et al, 2009, Masiero et al, 2007].
However, many of these results are contradictory, and not all robotic systems have undergone rigorous clinical testing [Rosati, 2010]. Furthermore, there is a lack of data showing improvements on measures related to *activities of daily living (ADL)* [Mehrholz et al, 2012], and some experimental evidence indicates that to date robotic training fails to transfer to improvement on the functional level [Timmermans et al, 2009]. This may be due to the fact that most of the existing robotic devices are programmed to produce simple stereotyped movements of the limbs, often not related to the functional activities included in measures ADL.

Further, many of the developed systems have been designed from an engineering perspective rather than based on therapy demands, and most rehabilitation paradigms are based on the repetition of stereotypical movements instead of applying more advanced principles of motor control and motor learning [Rosati, 2010].

A pathological subject may improve grip force with the force control system of almost all robotic rehabilitation devices but may not be able to use that force to pick up a jar [Richards et al, 1999].

Finally, the biomechanical parameters proposed until today in the scientific literature, to evaluate the quality of the movement, are related to the specific robot used and to the type of exercise performed and are still far to be considered as viable alternatives to the clinical scales and there is still lacking of a standardization of quantitative kinematic and dynamic indexes and rehabilitation protocols that are objectively more effective for the recovery of motor function.
As a result, the effectiveness of robotic rehabilitation is still being discussed [Rosati, 2010]. Even though to date there is not yet enough evidence to definitely confirm the efficacy of robotic therapy, the

development of these systems is still in an early stage and the potential of robotics in rehabilitation is still unexploited [Timmermans et al, 2009, Masiero et al, 2009].
The focus is to investigate, using new robust indexes, the *quality* of a reaching movement and to gain a better understanding of how kinematic and EMG patterns of the upper limb reaching movements are achieved in healthy subjects and how they changes in presence of some pathologies, and to apply this information to rehabilitation concepts.

6.2 Reaching movements in stroke disease

Understanding movement deficits following CNS lesions and the relationships between these deficits and functional ability is fundamental to the development of successful rehabilitation therapies (Lough *et al.*, 1984). The impairment of upper limb function is one of the most common and challenging sequelae following stroke, and it limits the patient's autonomy in activities of daily living and may lead to permanent disability (Nakayama *et al.*, 1994).
Movement deficits are most evident in the limb contralateral to the side of the stroke and are characterized by *weakness of specific muscles* (Bourbonnais and Vanden Noven, 1989); *abnormal muscle tone* (Wiesendanger, 1990); *abnormal movement synergies* (Bobath, 1990); lack of mobility between structures at the shoulder girdle (Ryerson and Levit, 1987).
In stroke subjects, goal-directed movements are characterized by *slowness, spatial and temporal discontinuity and abnormal patterns of muscle activation* (Gowland *et al.*, 1992; Levin, 1996*a*).

6.3 Design of the experiment

Here is proposed a quantitative kinematic and electromyographic assessment of robot assisted upper arm reaching. Particularly, we study the quality and the motor composition of visually-guided reaching movements from people with pathological conditions, applying the minimum jerk theory and the decomposition method proposed in section 4 to identify the sub-movements and to estimate the force muscle involved. For this study, 5 healthy subjects (50±8 year old, males) and 5 pathological subject (PS) (males, 45 years old). Inclusion criteria for the patients were the following: (1) diagnosis of a single, unilateral stroke at least 5 months prior to enrollment verified by brain imaging; (2) sufficient cognitive and language abilities to understand and follow instructions.

The protocol has been approved by the scientific technical committee of the Research Institute "Salvatore Maugeri Foundation", Benevento (Italy) and the written consent has been obtained from all subjects or their guardians.

The robotic device used in this study was the Multi-Joint-System (in the following MJS) of the Tecnobody. Its mechanical arm is provided with four "freedom" ranges, giving the patient freedom of joint movement in the three fundamental axes of movement (Anterior-Posterior, Adduction-Abduction, Internal rotation- External rotation).

Each subject underwent to two trial, each of them consisting of four horizontal reaching tasks (Figure . The task required each subject to move from the center position to the target and then return to the center with a sequence of four reaching movements RM (Table I), exploring the shoulder horizontal flexion (SHF) and horizontal extension (SHE). Subjects were instructed to perform movements at their natural speed.

Table I. Description of the four movements in horizontal reaching task

Task	Task Acronym	Meaning	Description
SHE	EH1	Extension Horizontal 1	Horizontal extension of the right shoulder from the middle position to the outer right
	EH2	Extension Horizontal 2	Horizontal extension of the right shoulder from the outer left position to the middle one
SHF	FH1	Flexion Horizontal 1	Horizontal flexion of the right shoulder from the right external position to the middle one
	FH2	Flexion Horizontal 2	Horizontal flexion of the right shoulder from the middle position to left external one

Moreover, subjects were instructed to make one continuous movement to avoid the possibility of having the subject break the task up into several discrete subtasks.

The electromyographic analysis consisted of eight EMG channels have been acquired by a wireless BTS Freemg 300 system with variable geometry mounting clip surfaces electrode, 16-bit resolution, 1 kHz sampling rate, in the 20-400 Hz frequency band, over the main muscles involved in the above described motor task and exactly: 1) clavicular major pectoralis, 2) Trapezius (middle fibers), 3) anterior and 4) posterior deltoid. These muscles were selected because of their synergistic and agonist/antagonist role, as explained in Table II:

Table II. Activated muscles for the shoulder motions.

Task	Agonist	Antagonist
SHE	Posterior Deltoid (PD) Trapezius (middle fibers) (TM)	Anteriod Deltoid (AD) Clavicular Pectoralis Major (CPM)
SHF	Clavicular Pectoralis Major Anterior Deltoid	Posterior Deltoid Trapezius (middle fibers)

All surface EMG recordings have been performed according to related SENIAM recommendation [European Recommendations for Surface ElectroMyoGraphy, deliverable of the SENIAM project. ISBN: 90-75452-15-2]. To avoid fatigue effects on EMG measurements, 1 min of rest was observed between trials. Kinematic and EMG data were recorded simultaneously.

During each trial, subjects were asked to seat on the ergonomic chair of the robot with the trunk erected, neck straight fixing the central green starting point on the front monitor (green circle with letter "H" in Figure 20).

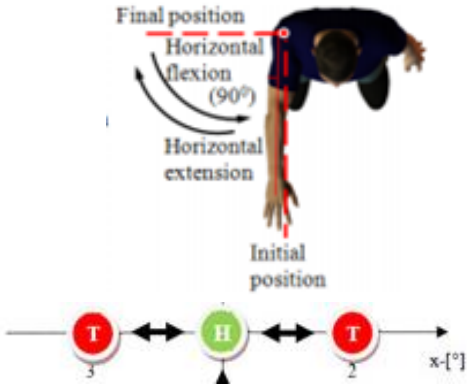

Figure 14. The visually-guided planar reaching task.

The arm under test holding the robot grip by the hand in a position parallel to the floor at 90° with the trunk, the arm not under test on side handle close to the seat. Kinematic task consists on a visually-guided planar reaching task. A targets were placed at 30° from the center target (really the arm reaches the final position covering a 30° angle) and visual feedback of both target and robot handle location were provided on a computer screen in front of the robot. Since the low Index of Difficulty (ID) of the task [Fitts, 1954], it is expected one continuous movement with one-peaked velocity profile approximately located between around the 50% of the reach.

6.4 Signal processing

Spatial coordinates of the handle position along x and y axes were analogically recorded with a 1/10° degree resolution and sampled at a sampling rate of 20 Hz. Velocity profiles have been computed using a derivative algorithm. Since differentiation degrades signal-to-noise ratio, the filter has to be carefully chosen.
To this aim has been used a Savitzky-Golay filter of third order and of frame length 41. Movement's onset/end times were calculated on the velocity profile in correspondence of successive zero crossing. In order to avoid to consider false positives, only zero crossings with an interval distance equal to the set angular excursion of the specific task were accepted.
Moreover, movement's onset/end times were used to identify the muscle activation zone corresponding to the muscular effort required for reaching movements.

6.5 Kinematic evaluation

The quality and accuracy of the movements have been described by smoothness index that is a typical kinematic measure in reaching movement studies [Jyh-Jong Chang et al, 2008; Zollo et al, 2011; Conroy et al, 2011; Teulings et al, 1997]. As it has been frequently observed, single-joint movements are characterized by single-peaked, bell-shaped speed profiles.
This finding and the tendency of natural movements to be characteristically smooth and graceful, led to suggest the motor coordination can be mathematically modelled by postulating the voluntary movements are made, at least in the absence of any other overriding concerns, to be as smooth as possible.

In according with this theory, smoothness is based on the minimum jerk theory stating that any single-joint movement can be described by a fifth order polynomial p(t) of the form [Flash et al, 1985]:

$$\mathrm{p(t)} = \mathrm{I} + \mathrm{F}\{10(t/T)^3 - 15(t/T)^4 + 6(t/T)^5\}$$

where F is the final position at time T (end of the movement).

To produce a maximum smoothness movement, one must minimize the jerk cost functional defined as;

$$J = \int_{t_0}^{t_f} \left(\frac{d^3\Theta}{dt^3}\right)^2$$

where Θ is the angular displacement. Jerk is the rate of the change of acceleration with respect to time (third time derivative of the position). To test the hypothesis that movements to different targets and/or of different duration were simply scaled replicas of a standard movement, normalized smoothness is considered.
Several different ways to normalize jerk-based measures have been used to reduce dependency on those variables [D'Addio G. et al, 2012]. In this study, it has been considered the following normalized smoothness (NS) [33]

$$J = \frac{D^5}{A^2} \int_0^d \left|\frac{d^3\Theta}{dt^3}\right|^2 dt$$

where A is the movement amplitude and D its duration. The quality of the movement is evaluated introducing the kinematic index ***Level of Smoothness (SL)*** defined as follows:

$$SL = \frac{J_m - J_i}{Ji}$$

where J_m is the NS measured on the subject's reaching movement (or real reaching movement) while J_i is the NS obtained considering the

ideal movement extracted by the minimum jerk theory with p(0)=0 and p(T)=30°.

The lower the relative error, the greater the quality of the measurement. A zero-value for the SL is related to a perfect match between the quality of the movement performed by the subject and the quality of the movement predicted by the mathematical minimum jerk model. Velocity profiles of each measured reaching movement are modelled as summation of Gaussian pulses according to the algorithm described in section 4.

To analyze the motor strategy of the subjects we have considered:

(I) the ***number (N)*** of each sub-movement that is regarded as the number of consecutive motion units to be gradually produced to reach the target

(II) **Temporal duration** (TD) of each sub-movement, expressed in % of the entire movement

6.6 Electromyographic evaluation

The acquired EMG signals have been: 1) high-pass filtered forward and backward (zero phase distortion) at 10 Hz to remove motion artifact, 2) full wave rectified, and 3) then low-pass filtered forward and backward (zero phase distortion) at 5 Hz to create the linear envelope (LE) of the rectified EMGs. Algorithms usually proposed consider a muscle activation in case of an EMG amplitude higher than baseline resting activity plus 3 times its standard deviation for about 30 ms. However, this solution does not fit the muscular effort required to initially hold the arm in the exercise starting position, leading to a confounding identification of activation/deactivation muscle's patterns.

To overcome the above problem, concerning the baseline activity epoch selection, the LEs of the studied muscles are segmented considering the onset and end times of the several movements (EH1, EH2, IH1, IH2) on the kinematic signals. In this way, only these portions of LEs are examined (Figure 21 and 22).

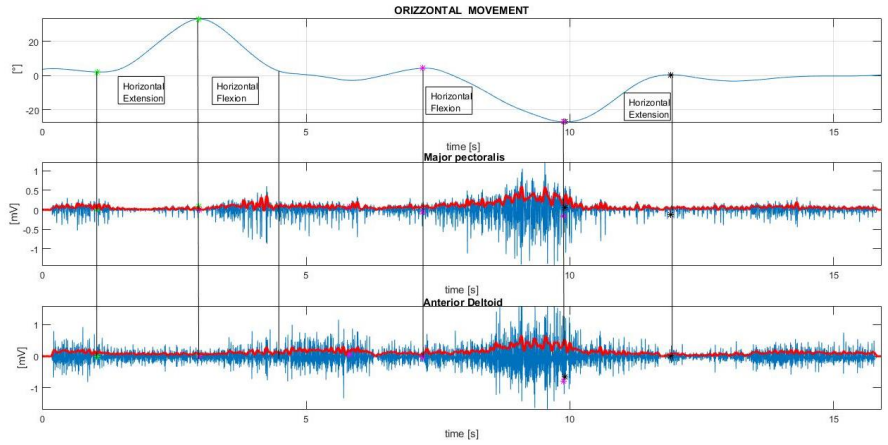

Figure 21. Example of the raw EMG signals of the flexor muscles with their Les. The vertical lines are the temporal markers between the different kinematic tasks (extension and flexion movements).

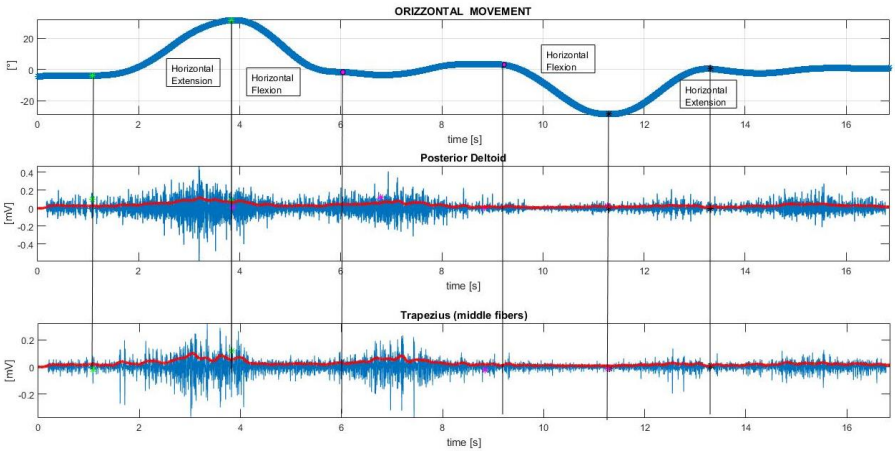

Figure 152. Example of the raw EMG signals of the extensor muscles with their Les. The vertical lines are the temporal markers between the different kinematic tasks (extension and flexion movements).

Then, it is considered an *amplitude normalization* of all Les by peak dynamic method (PDM) [Mathiassen et al, 1990], a method that still appears to be popular among gait electromyographers [Mirka, 1991; Yang J. et al, 1984], dividing each point that constitutes the processed EMG by the peak value of the same EMG.

Further, has been considered a *time normalization* of Les by linear interpolation or decimation to reconstruct each signal epoch with the same number of 1024 data points (for a sampling rate of the EMG signal of 1 kHz). The original time scale is then converted in "percent of cycle" ranging from 0 to 100% of the motor task.

Each LE is modelled as summation of Gaussian pulses according to the algorithm described in section 4. Aim of this decomposition is to identify *temporal features* of the EMG LE, such as the amplitude, the time of occurrence, and the duration of the *EMG phasic activity* during the arm movement.

As shown in literature [Van Hedel et al, 2006], the decomposition of the LE usually generates an high number of *phasic activity* (here named M), so, to simplify EMG LE representation, only the *dominant phasic activity* from each LE are considered. The *dominant phases* are defined as the phases of activity which have a significant percentage of the area [Van Hedel et al, 2006] and they are estimated by means of two steps.

First, macro activations areas are automatically detected as the intervals where the LE exceeds a threshold, equal to its mean value plus three times its standard deviation, for at least 50 ms and therefore identifying EMG LE ON-OFF times.

Then, another threshold is defined as the sum of the LE areas under the macro-activations divided by M-1. All the phasic activity with area higher than this threshold are defined as *dominant phases.* By using only the dominant phases of each LE and disregarding the remaining phases of that LE, the unnecessary data are removed. The dominant phase with the largest $\boldsymbol{\alpha_i}$ attribute is further defined as the *peak activity or peak phase (PA) of the LE*.

The other dominant phases are called *major phases* (Figure 23). In the following we will use the acronym PA also to indicate the position of peak value of the PA, expressed in percentage of the task motor.

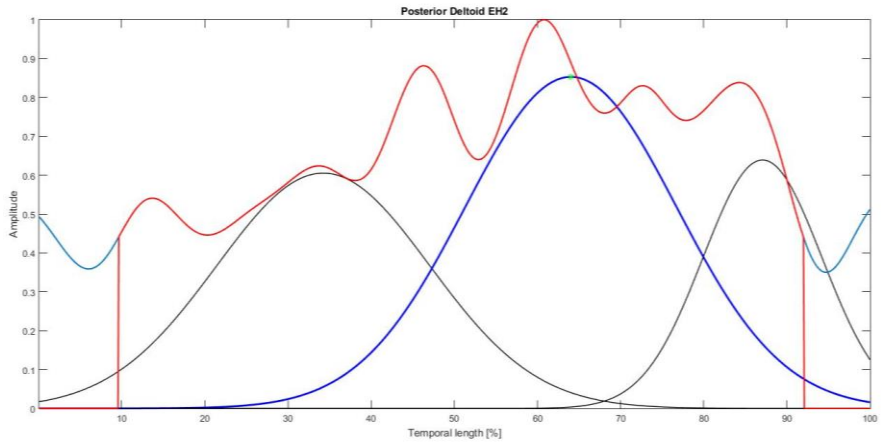

Figure 23. Example of the analysis of the posteriorr deltoid over the second horizontal flexion (EH2). The red line represents the activation zone of the LE; the PA is represented in blue line and the major phases in black lines.

6.7 Results

Differences among the SL, sub-movements features and PA values within control and pathological groups have been compared using the Mann-Withney test (independent samples).
A total of 80 (4*2*5*2) RM have been recorded. In Figure 24 and 25 are reported the trajectories, the velocity , the acceleration and jerk profiles of two representative subjects from the comparison group, and of two representative stroke patients during the point-to-point evaluation task.

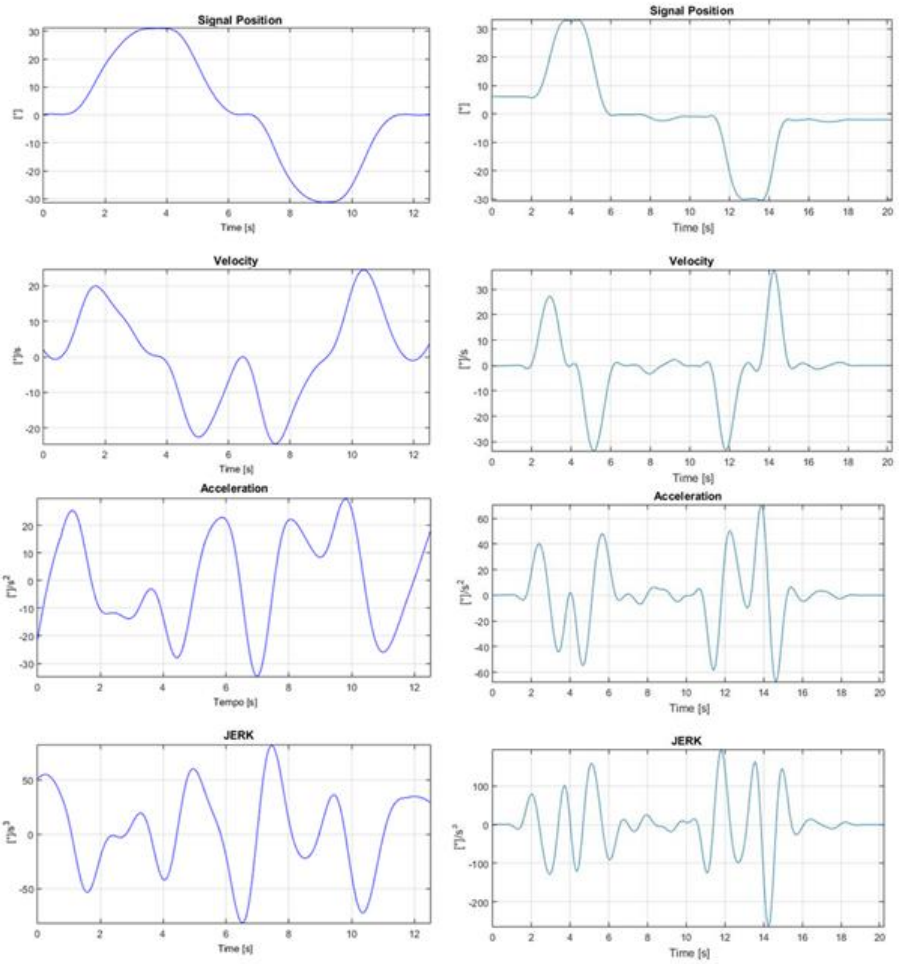

Figure 24. The trajectory[°], velocity[°/s], acceleration[°/s^2] and jerk[°/s^3] profiles for two representative control subjects during a complete trial. On the x-axis are reported the time [s].

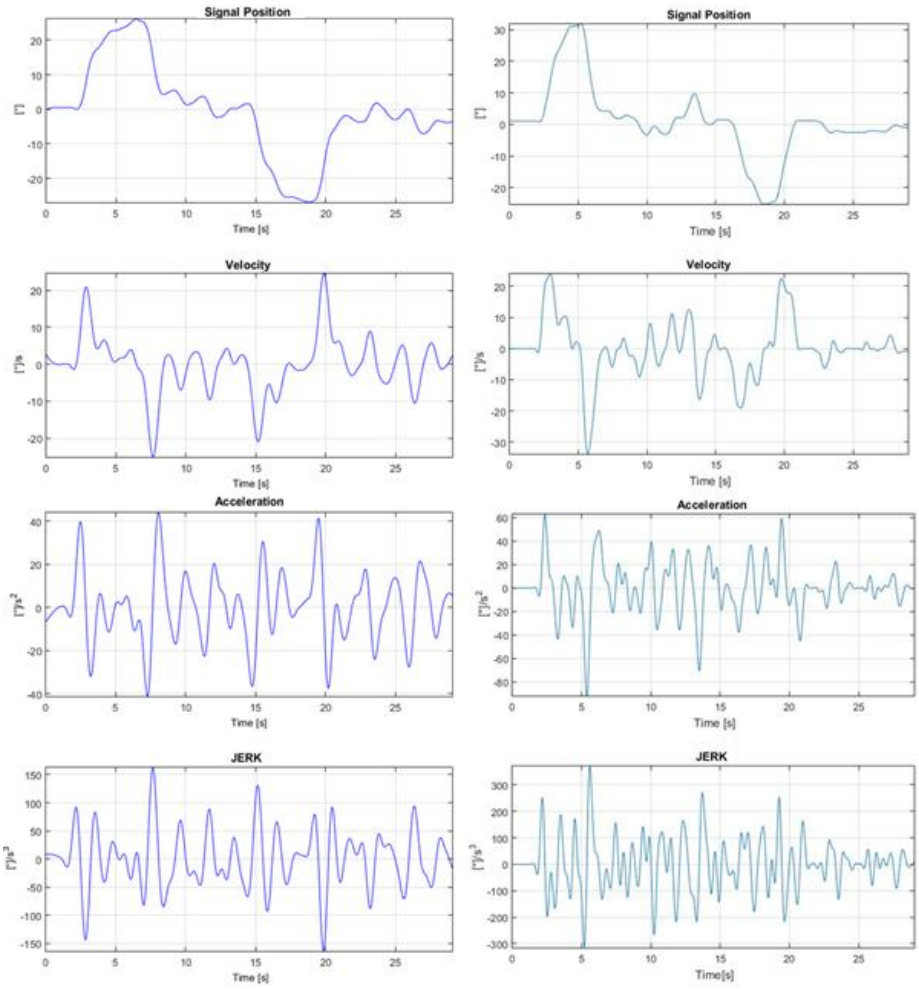

Figure 25. The trajectory[°], velocity[°/s], acceleration[°/s^2] and jerk[°/s^3] profiles for two representative stroke subjects during a complete trial. On the x-axis are reported the time [s].

As was to be expected, the movements of the pathological subjects are more fragmented and less continuous. Particularly, it can possible to note several peaks in the velocity profile, typical behavior in stroke disease. In Figure 26 and 27 are represented, respectively, the decomposition of the velocity profiles of each horizontal task for one healthy and one pathological subject.

The original time scale is then converted in "percent of movement" ranging from 0 to 100% of the entire movement.

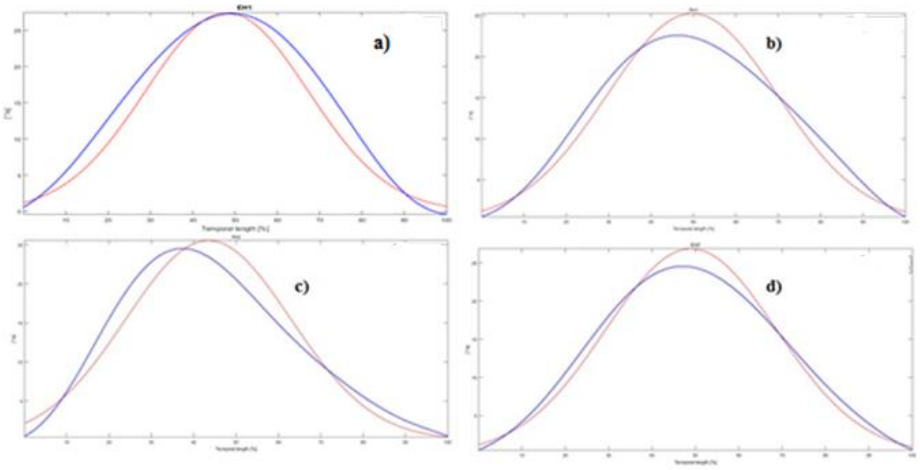

Figure 26. Sub-movements composition of the arm movement into Gaussian components for one representative control subject. a) EH1; b) FH1; c) FH2; d) EH2. On the x-axis is reported the temporal length of the movement expressed in %. On the y-axis the velocity [°/s].

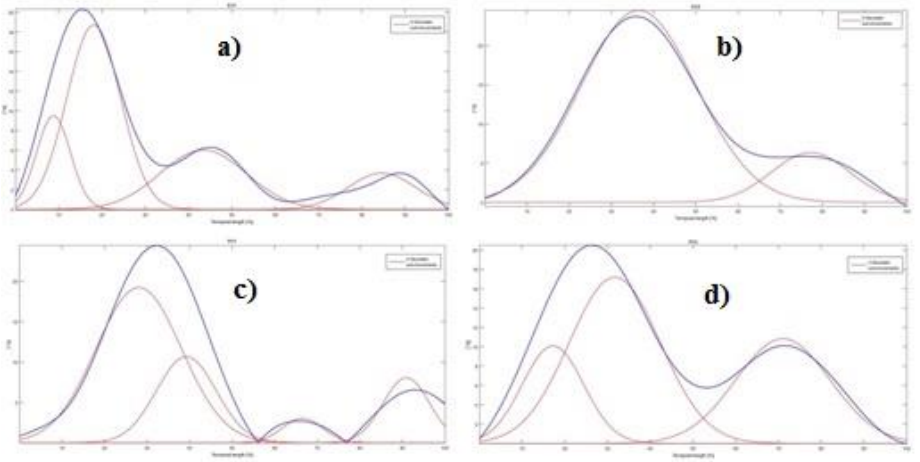

Figure 27. Sub-movements composition of the arm movement into Gaussian components for one representative pathological subject. a) EH1; b) FH1; c) FH2; d) EH2. On the x-axis is reported the temporal length of the movement expressed in %. On the y-axis the velocity [°/sec].

As to was expected, the velocity profiles of the healthy subjects, are very close to the uni-modal and bell-shaped profiles predicted by the minimum-jerk model. Moreover, the peak velocitv occurred around the 55% of the reach, which has been reported for unimpaired reaching to target (Bullock & Grossberg, 1988; Hogan, 1984; Hollerbach & Flash, 1982; Morasso, 1983: Soechting & Lacquaniti, 1981).

We found a single sub-movement in 95% of the analysed trials. In pathological conditions, there were significantly more movement units, indicating that the continuous strategy was lost. The velocity profile performed by pathological subjects exhibit multiple peaks which indicate that the movements are produced by repetitive accelerations and decelerations. In table III are reported the results of the kinematic evaluations related to the SHE task (EH1 and EH2) and to the SHF (FH1 and FH2) for both healthy and hemiparetic subjects, respectively HS and PS.

Table III. Kinematic indices for both healthy and pathological motion tasks

	Task	***SL (mean ±SD)***	***TD(mean ±SD)***	***N (mean ±SD)***
Healthy subjects	*SHE*	0.80 ± 0.50	100	1 ± 0
	SHF	0.51 ± 0.48	100	1 ± 0

	Task	***SL (mean ±SD)***	***TD (mean ±SD)***	***N (mean ±SD)***
Pathological subjects	*SHE*	24 ± 20	45 ± 11	4 ± 1
	SHF	18 ± 17	49 ± 13	3 ± 1

As shown in figure 28 and 29, the comparison of kinematic indices indicated a considerable difference between HS and PS. Moreover it was observed higher values during the SHE than the SHF although this comparison did not reach significance according. This indicates that the PS showed more difficult to perform an extension reaching movement than a flexion movement.

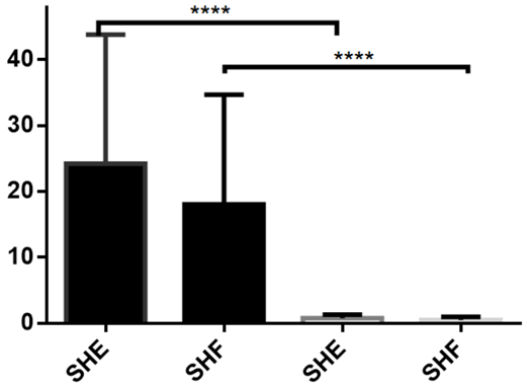

Figure 28. Smoothness Level for the SHE and SHF tasks for both HS (white bars) and PS (black bars); p<0.0001**** indicates highly significant differences.

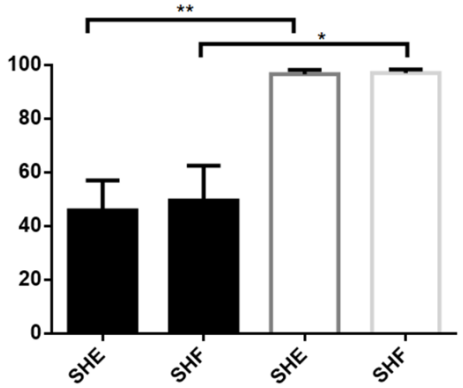

Figure 29. Total duration of the sub-movements for the SHE and SHF tasks for both HS (grey bars) and PS (black bars); p<0.05* and p<0.01** indicate respectively significant and very significant differences.

In order to evaluate the muscle activation timing and the muscle forces, the distribution of the occurrences the peak phase has been reported for each muscle. The distributions refer to all the RM and all the studied muscles in a group (Figure 30).

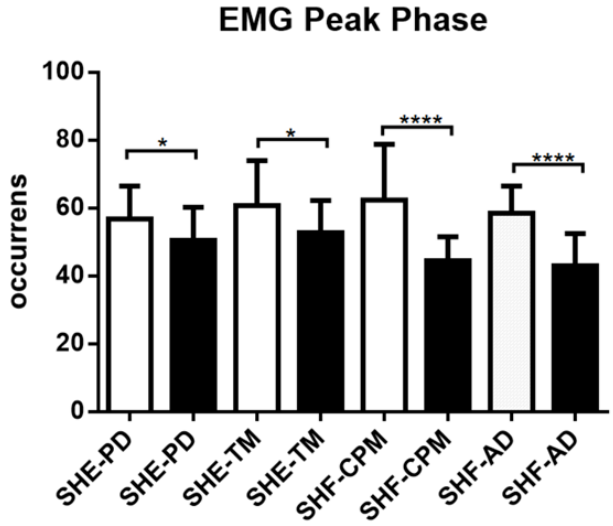

Figure 30. Distribution of the occurrences of the Peak Phase referred to the normalised EMG LEs of all the studied muscles and all the RM. SHE: Shoulder Horizontal Extension; SHF: Shoulder Horizontal Flexion; PD=posterior deltoid; TM: Trapezius (middle fibers); CPM: Clavicular Pectoralis Major; AD= Anterior Deltoid. Black bars: PS; White bars: HS.

For the healthy subjects the peak phases the extensor (PD and TM) and flexors (CPM and AD) muscles substantially lie in the middle / terminal part of each movement. The distributions for both the PD/TM and CPM/AD couple muscles are very similar, suggesting an extensor and a flexor synergy. For pathological patients the distribution of the peak phases occurs early. This reveals a global advance in maximum muscle effort compared to the healthy subjects. These behaviours are due to the inability of the pathological subjects to correctly plan and to keep a normal muscle synergy during the entire movement.

Discussions

Several studies have showed the importance of a clear understanding of arm movements. Studies of kinematic, mechanical, and neural features of arm reaching movements agree that, in the absence of any overriding requirement such as maximum speed or precision, their typical characterization consists in to be a straight path with a Gaussian-like bell shaped velocity profile (minimum jerk theory). However, several studies noted that more complex reaching movements or movements under constraints of time and spatial accuracy are often characterized by irregular and asymmetric multi-peaked velocity profiles. These experimental evidences led to the emergence of the theory of the discretization of the movement.

There is a wide number of studies on human motor control supporting the theory that reaching and pointing movements are the result of sequences of discrete motion units, called *sub-movements*. Identifying fundamental building blocks that underlie human movement is a major goal of motor control studies. If such a structure could be identified and accurately characterized, it would provide the ability to scrutinize human movement at a deeper level than has been previously possible.

Moreover, considering any movement as a combination of "primitive" blocks leads to a interesting theory that lends itself well to a mathematical application, especially for the striking analogy with the Fourier approach.

As a non-linear optimization problem, the sub-movement problem may have multiple local minima. However, several optimization methods applied to overcome this problem are sensitive to getting caught in local minima and cannot guarantee a globally optimal solution. The optimality of the solution for these methods depends heavily on the quality of the initial guess; unless the initial guess is in the neighborhood of the global minimum, they will not find the best solution. In order to reliably find the global minimum and solve the decomposition problem accurately, an algorithm capable of global nonlinear optimization is necessary.

Here is proposed a novel sub-movement decomposition method based on a robust EM constrained algorithm which assurances a globally optimal solution. In fact we overcome the critical aspects of the EM algorithm such as the parameters initialization and determination of the number of components composing a finite mixture. Particularly, it has been realized an hybrid decomposition algorithm between a purely local and a purely global optimization algorithm.

This representation allowed to explore whether the movements are built up of elementary kinematic units by decomposing each surface into a weighted combination of Gaussian functions. The proposed method has been capable of finding the optimal decomposition for simulated velocity data. These issues are particularly felt in the sub-movements theory where the shape and the number of building blocks composing a motor task is not known.

Then, applying this new decomposition algorithm it have been defined new robust kinematic and electromyographic indexes to analyze the strategy of the reaching movements in hemiparetic subjects during a robot based rehabilitation of upper arm.

The obtained results indicated that the decomposition method proposed in addition to the SL and PP indexes allowed us to meaningfully investigate the motor strategy of movement produced by subjects with hemiparesis.

References

Abend, W., Bizzi, E., and Morasso, P. (1982). Human arm tra jectory formation. Brain, 105:331{348

Arrow K. J. and L. Hurwicz. Gradient method for concave programming, I: Local results. In K. J. Arrow, L. Hurwica, and H. Uzawa, editors. Studies in Linear and Nonlinear Programming. Stanford University Press, Stanford, CA, 1958.

Babaud, A. Witkin, and R. Duda, "Uniqueness of the Gaussian kernel for scale-space filtering," IEEE Trans. Pattern Anal. Mach. Intell., vol. PAMI-8, pp. 26-33, Jan. 1986.

Baldi. P. Gradient descent learning algorithm overview, a general dynamical systems perspective. IEEE Transactions on Neural Networks, 6(1):182-195, January 1995.

Bernstein, N. (1967). The co-ordination and regulation of movements. Oxford, UK: Pergamon Press. n. 97.

Berthier NE (1997) Analysis of reaching for stationary and moving objects in the human infant. In: Donahue J, Dorsal VP (eds) Neural network models of complex behavior – biobehavioral foundations. North-Holland, Amsterdam, pp 283–301.

Berthier Neil E.. Learning to reach: A mathematical model. Developmental Psychology, 32(5):811–823, 1996.

Bilodeau, M. et al. (2003). EMG frequency content changes with increasing force and during fatigue in the quadriceps femoris muscle of men and women. Journal of Electromyography and Kinesiology, Vol.13, No.1, Feb. 2003, pp.83-92, ISSN 1050-6411.

Bobath B. Adult hemiplegia. Evaluation and treatment. 3rd ed. Oxford: Heinemann Medical; 1990.

Bohannon RW, Smith MB. Interrater reliability of a modified Ashworth scale of muscle spasticity. Phys Ther 1987; 67: 206–7.

Bullock, D.. & Grossherg, S. (1988), Neural dynamics of plarlnell aml movements: Emergent invarients and sreedaccur,\l'V

properties during trajectory formation. f'.\l'chological Nel'iew, 95, 49-90.

Burdet E and Milner TE. Quantization of human motions and learning of accurate movements. Biological Cybernetics, 78: 307–318, 1998.

Carr JH, Shepherd RB. A motor relearning program for stroke. 2nd ed. Rockville (MD): Aspen; 1987b.

Chen and B.Luo, "Robust T-mixture Modeling with SMEM Algorithm" , Proceedings of the Third International Conference on Machine Learning and Cybernetics, Shanghai, pp. 3689-3694, August 2004.

Chen JJ1, Shiavi RG, Zhang LQ. A quantitative and qualitative description of electromyographic linear envelopes for synergy analysis. IEEE Trans Biomed Eng. 1992 Jan;39(1):9-18.

Chen Scott Shaobing, David L. Donoho, and Michael A. Saunders. Atomic decomposition by basis pursuit. SIAM Journal of Scientific Computing, 20(1):33– 61, 1998.

Collewijn H, Erkelens CJ, Steinman RM, Binocular coordination of human horizontal saccadic eye movements, Journal of Physiology, vol. 404, 1988, pp. 157-182.

Conroy SS, Whitall J, Dipietro L, Jones-Lush LM, Zhan M, Finley MA, Wittenberg GF, Krebs HI, Bever CT., "Effect of gravity on robot-assisted motor training after chronic stroke: a randomized trial", Arch Phys Med Rehabil. 2011 Nov;92(11):1754-61. doi: 10.1016/j.apmr.2011.06.016. Epub 2011 Aug 17.

Crossman ERFW, Goodeve PJ (1983) Feedback control of hand movement and Fitts' Law. Q J Exp Psychol A 35:251–278.

Cybenko, G. (1989) Math. Control Signal System 2, 303–314.

D. Luca C.. The use of surface electromyography in biomechanics," J Appl Biomech, vol. 13, no. 2, pp. 135{163, 1997.

D'Addio G., Cesarelli M., Romano M., De Nunzio A., Lullo F. and Pappone N.. EMG Patterns in Robot Assisted Reaching Movements of Upper Arm. 5th European Conference of the

International Federation for Medical and Biological Engineering IFMBE Proceedings Volume 37, 2012, pp 749-75.

Dantzig. G. B. Linear Programming and Extensions_ Princeton University Press. 1963.

Davidson P. R., Jones R. D., Sirisena H. R., and Andreae J. H., "Detection of adaptive inverse models in the human motor system," Hum. Mov. Sci., vol. 19, no. 5, pp. 761–795, 2000.

Dipietro L, Krebs HI, Volpe BT, and Hogan N. Combinations of elementary units underlying human arm movements at different speeds. Proceedings of the Society for Neuroscience, 2004.

Dipietro L., Hermano I. Krebs, Susan E. Fasolid, Bruce T. Volpe and Neville Hogan, Sub-movement changes characterize generalization of motor recovery after stroke, Cortex, Volume 45, Issue 3, March 2009, Pages 318-324.

Doeringer JA and Hogan N. Intermittency in preplanned elbow movements persists in the ab-sence of visual feedback. The Journal of Neurophysiology, 80: 1787–1799, 1998.

Doeringer Joseph A.. An Investigation into the Discrete Nature of Human Arm Movements. PhD thesis, Massachusetts Institute of Technology, 1999.

Dounskaia, N.,Kinematic invariants during cyclical arm movements, Biological Cybernetics, vol. 96, 2007, pp. 147–163.

European Recommendations for Surface ElectroMyoGraphy, deliverable of the SENIAM project. ISBN: 90-75452-15-2.

Fasoli SE, Krebs HI, Stein J, Frontera WR, Hogan N., "Effects of robotic therapy on motor impairment and recovery in chronic stroke", Arch Phys Med Rehabil., 84(4):477-82, 2003.

Figueiredo M.A.T., and Jain A.K., "Unsupervised learning of finite mixture models", IEEE Trans Pattern Analysis and Machine Intelligence, Vol. 24, No.3, pp.381-396,2002 March.

Fitts MP, The information capacity of the human motor system in controlling the amplitude of movement, J Exp Psychol. 1954 Jun;47(6):381-91.

Flash T, Henis E. Arm trajectory modifications during reaching towards visual targets. J Cogn Neurosci. 1991 Summer;3(3):220-30. doi: 10.1162/jocn.1991.3.3.220.

Flash, T., & Hogan, N. (1985). The coordination of arm movements: An experimental confirmed mathematical model. Journal of Neurosciences, 7, 1688–1703.

Flash, T., & Sejnowski, T. J. (2001). Computational approaches to motor control. Current Opinion in Neurobiology, 11, 655–662.

Florack L. M. J., B. M. ter Haar Romeny, J. J. Koenderink, and M. A. Viergever. Linear scale-space. Journal of Mathematical Imaging and Vision, 4(4):325–351, 1994. 2, 2; 768, 1984.

Floudas C. A. and P. M. Pardalos. A Collection of Test Problems for Constrained Global Optimization Algorithms, volume 455 of Lecture Notes in Computer Science, Springer-Verlag, 1990.

Floudas C. A. and Pardalos P. M. . A Collection of Test Problems for Constrained Global Optimization Algorithms, volume 455 of Lecture Notes in Computer Science. Springer, Verlag_ 1990.

Floudas C. A. and Visweswaran V. Quadratic optimization. In Reiner Horst and P. M. Pardalos, editors, Handbook of Global Optimization, pages 217-269. Kluwer Academic Publishers, 1995.

Gorse D. and A. Shepherd. Adding stochastic search to conjugate gradient algorithms. In Proc. of the 3rd Intl Conf on Parallel Applications in Statistics and Economics, Prague, Tifkarenfke Zacody, 1992.

Gowland C, deBruin H, Basmajian JV, Plews N, Burcea I. Agonist and antagonist activity during voluntary upper-limb movement in patients with stroke. Phys Ther 1992; 72: 624–33.

Gowland C, Stratford P, Ward M, Moreland J, Torresin W, Van Hullenaar S, et al. Measuring physical impairment and disability with the Chedoke–McMaster Stroke Assessment. Stroke 1993; 24: 58–63.

Gregor, SM. et al. (2002). Lower extremity general muscle moment patterns in healthy individuals during recumbent cycling. Clinical Biomechanics, Vol.17, No.2, Feb. 2002, pp.123-129, ISSN 0268-0033.

Griewank A. O.. Generalized descent for global optimization. Journal of Optimization Theory and Applications, 34:11-39, 1981.

Gross, J., Timmermann, L., Kujala, J., Dirks, M., Schmitz, F., Salmelin, R., Schnitzler, A., The neural basis of intermittent motor control in humans, Proc Natl Acad Sci, vol. 99, 2002, pp. 2299–2302.

Guigon, E., Baraduc, P., & Desmurget, M. (2007). Computational motor control: redundancy and invariance. Journal of Neurophysiology, 97: 331–347.

Guimarães, AC. et al. (1994). EMG-force relationship of the cat soleus muscle studied with distributed and non-periodic stimulation of ventral root filaments. Journal of Experimental Biology, Vol.186, No.1, Jan.1994, pp.75-93, ISSN 0022-0949.

H. Krebs, \Robot Mediated Movement Therapy: A Tool for Training and Evaluation," in Eur Symp Tech Aids Rehabil - TAR 2007, Technical University of Berlin, 2007.

Harwin W., J. Patton, and V. Edgerton, \Challenges and Opportunities for Robot-Mediated Neurorehabilitation," Proc IEEE, vol. 94, no. 9, pp. 1717{1726, Sept. 2006.

Hogan N (1984). An organizing principle for a class of voluntary movements. J Neurosci 4: 2745-54.

Hogan,N. and Sternad,D.(2012). Dynamic primitives of motor behavior. Biol. Cybern. 106, 727–739.doi:10.1007/s00422- 012-0527-1.

Hollerbach,)., & Flash, T (1982). DynamiC interactions between limb segments during planar arm movement. Biological C)'heme!ics, 44, 67-77.

Hornik, K., Stinchcombe, M.&White, H. (1989) Neural Network 2, 359–366.

Horst R. and H. Tuy. Global optimization: Deterministic approaches. Springer-Verlag, Berlin, 1993.

Horst Reiner and Pardalos P. M., editors. Handbook of Global Optimization. Kluwer Academic Publishers, 1995.

Jaggi Seema, William C. Karl, Stephane Mallat, and Alan S. Willsky. High resolution pursuit for feature extraction. Technical Report LIDS-P-2371, Laboratory for Information and Decision Systems, Massachusetts Institute of Technology, November 1996.

Jyh-Jong Chang, Yu-Sheng Yang, Wen-Lan Wu, Lan-Yuen Guo, Fong-Chin Su, "The Constructs of Kinematic Measures for Reaching Performance in Stroke Patients", J. of Med. and Biol. Eng., Vol 28, No 2 (2008).

Kandel, E., JH, J. S., & Jessell, T. (Eds.). (2000). Principles of neural science (Fourth ed.). McGraw Hill.

Karlsson, S.; Gerdle, B. (2001). Mean frequency and signal amplitude of the surface EMG of the quadriceps muscles increase with increasing torque – a study using the continuous wavelet transform. Journal of Eletromyography and Kinesiology, Vol.11, No.2, Apr. 2001, pp.131-140, ISSN 1050-6411.

Kinsella J. A. . Comparison and evaluation of variants of the conjugate gradient methods for efficient learning in feed-forward neural networks with backward error propagation. Neural Networks, 3:27-35, 1992.

Krebs Hermano Igo. Robot-Aided Neurorehabilitation and Functional Imaging. PhD thesis, Massachusetts Institute of Technology, 1997.

Krebs HI, Aisen ML, Volpe BT, Hogan N (1999) Quantization of continuous arm movements in humans with brain injury. Proc Natl Acad Sci USA 96:4645–4649.

Lashley KS. Integrative function of the cerebral cortex. Physiol Rev 13: 1–42, 1933.

Lee, D., Port, N.L., Georgopoulos, A.P., Manual interception of moving targets. II. Online control of overlapping sub-movements, Experimental Brain Research, vol. 116, 1997, pp. 421–433.

References

Levin MF. Interjoint coordination during pointing movements is disrupted in spastic hemiparesis. Brain 1996a; 119: 281–93.

Levin MF. Interjoint coordination during pointing movements is disrupted in spastic hemiparesis. Brain 1996a; 119: 281–93.

Lough S, Wing AM, Fraser C, Jenner JR. Measurement of recovery of function in the hemiparetic upper limb following stroke: a preliminary report. Hum Mov Sci 1984; 3: 247–56.

Lough, S., Wing, A.M., Fraser, C., Jenner, J.R. Measurement of recovery of function in the hemiparetic upper limb following stroke: A preliminary report (1984) Human Movement Science, 3 (3), pp. 247-256.

M. Rucci, D. Bullock, and F. Santini, Integrating robotics and neuroscience: brains for robots, bodies for brains, Advanced Robotics, vol. 21, 2007, pp. 1115–1129.

MacKenzie, I. S. (1991). Fitts' law as a performance model in human-computer interaction. Unpublished Doctoral Dissertation, University of Toronto.

Madeleine, P. et al. (2000). Mechanomyography and electromyography force relationships during concentric, isometric and eccentric contractions. Journal of Electromyography and Kinesiology, Vol.10, No.1, Feb. 2000, pp.33-45, ISSN 1050-6411.

Mallat S and Zhang Z. Matching pursuit with time-frequency dictionaries. IEEE Transactions on Signal Processing, 1993.

Marchal-Crespo L., Reinkensmeyer D., "Review of control strategies for robotic movement training after neurologic injury", J Neuroeng Rehabil., 6: 20, 2009.

Marotta, J. J., Medendorp, W. P., & Crawford, J. D. (2003). Kinematic rules for upper and lower arm contributions to grasp orientation. Journal of Neurophysiology, 90: 3816– 3827.

Masiero S., A. Celia, G. Rosati, and M. Armani, \Robotic-assisted rehabilitation of the upper limb after acute stroke." Arch Phys Med Rehabil, vol. 88, no. 2, pp. 142{9, Feb. 2007.

References

Masiero S., E. Carraro, C. Ferraro, P. Gallina, A. Rossi, and G. Rosati, \Upper limb rehabilitation robotics after stroke: a perspective from the University of Padua, Italy." J Rehabil Med, vol. 41, no. 12, pp. 981{5, Nov. 2009.

Mathiassen S. & Winkel J. (1990). Electromyographic activity in the shoulder-neck region according to arm position and glenohumeral torque. European Journal of Applied Physiology and Occupational Physiology, 61 5, 370-379.

Mehrholz J, Hädrich A, Platz T, Kugler J, Pohl M., "Electromechanical and robot-assisted arm training for improving generic activities of daily living, arm function, and arm muscle strength after stroke", Cochrane Database Syst Rev. 2012.

Meyer DE, Abrams RA, Kornblum S, Wright CE, Smith JE (1988) Optimality in human motor performance: ideal control of rapid aimed movements. Psychol Rev 95:340–370.

Meyer DE, Smith JE, Wright CE (1982) Models for the speed and accuracy of aimed movements. Psychol Rev 89:449–482.

Milner TE and Ijaz MM. The effect of accuracy constraints on three-dimensional movement kinematics. Neuroscience, 35: 365–374, 1990.

Milner TE and Ijaz MM. The effect of accuracy constraints on three-dimensional movement kinematics. Neuroscience, 35: 365–374, 1990.

Milner TE. A model for the generation of movements requiring endpoint position. Neurosci-ence, 49: 487–496, 1992.

Mirka G. A. (1991). The quantification of EMG normalization error. Ergonomics, 34 3, 343 – 352.

Mor~lsso, P. (1983). Three dimensional arm trajectories. Biological Cl'beme/ics, 48, 187-194.

Morasso P and Mussa-Ivaldi FA. Trajectory formation and handwriting: a computational mod-el. Biological Cybernetics, 45: 131–142, 1982.

References

Nakayama H, Jorgensen HS, Raaschou HO, Olsen TS. Recovery of upper extremity function in stroke patients: the Copenhagen Stroke Study. Arch Phys Med Rehabil 1994; 75: 394–8.

P. M. Pardalos and J. B. Rosen. Constrained Global Optimization: Algorithms and Applications, volume 268 of Lecture Notes in Computer Science. Springer-Verlag, 1987.

Parker R. G. and Rardin R. L.. Discrete Optimization. Academic Press. Inc., San Diego, CA, 1988.

Poggio, T. & Girosi, F. (1990) Science 247, 978–982.

Richards L., Pohl P., Therapeutic interventions to improve upper extremity recovery and function. Clin Geriatr Med. 1999 Nov;15(4):819-32.

Rohrer B, Fasoli S, Krebs HI, Hughes R, Volpe B, Frontera WR, Stein J, Hogan N. Movement smoothness changes during stroke recovery. J Neurosci. 2002 Sep 15;22(18):8297-304.

Rohrer, B.,and Hogan,N. (2003). Avoiding spurious sub-movement decompositions :a globally optimal algorithm. Biol. Cybern. 89, 190–199. doi:10.1007/s00422-003- 0428-4.

Rohrer,B., Hogan, N., Avoiding Spurious Sub-movement Decompositions II: A Scattershot Algorithm, Biological Cybernetics, vol. 94, 2006, pp. 409–414.

Rosati G., \The place of robotics in post-stroke rehabilitation." Expert Rev Med Devices, vol. 7, no. 6, pp. 753{8, Nov. 2010.

Ryerson S, Levit K. The shoulder in hemiplegia. In: Donatelli R, editor. Physical therapy of the shoulder. New York: Churchill Livingstone; 1987. p. 105–31.

Shadmehr R. and Wise S. P., The Computational Neurobiology of Reaching and Pointing: A Foundation for Motor Learning. Cambridge, MA, USA: MIT Press, 2005.

Smith and Jason Eisner. 2006. Annealing structural bias in multilingual weighted grammar induction. In Proc. of COLING-ACL, pages 569–576, July.

References

Soechting,). F., & La(quaniri, F. (1981). Invarianr (haracreristi(s of a pointing movement in man. journal 0/ Neuroscience, I, 710-720.

Spitkovsky, Hiyan Alshawi, and Daniel Jurafsky. 2010a. From baby steps to leapfrog: How Less is more in unsupervised dependency parsing. In Proc. of HLT-NAACL, pages 751–759. Association for Computational Linguistics, June.

Sturua E. G. and S. K. Zavriev. A trajectory algorithm based on the gradient method I. the search on the quasi-optimal trajectories. Journal of Global Optimization, 1991 (4): 375-388, 1991.

Teulings HL , Contreras-Vidal JL , Stelmach GE , Adler CH, “Parkinsonism reduces coordination of fingers, wrist, and arm in fine motor control”, Exp Neurol. 1997 Jul;146(1):159-70.

Timmermans A. a. a., H. a. M. Seelen, R. D. Willmann, and H. Kingma, \Technology-assisted training of arm-hand skills in stroke: concepts on reacquisition of motor control and therapist guidelines for rehabilitation technology design." J Neuroeng Rehabil, vol. 6, no. Figure 1, p. 1, Jan. 2009.

Todorov, E., & Jordan, M. (1998). Smoothness maximization along a predefined path accurately predicts the speed profiles of complex arm movements. Journal of Neurophysiology, 80, 696–714.

Todorov, E., & Jordan, M. (2002). Optimal feedback control as a theory of motor coordination. Nature 5(11).

Trombly CA. Deficits of reaching in subjects with left hemiparesis a pilot study. Am J Occup Ther 1992; 46: 887–97.

Uno, Y., Kawato, M., & Suzuki, R. (1989). Formation and control of optimal trajectory in human multijoint arm movement—Minimum torque change model. Biologic Cybernetics, 61: 89–101.

Vallbo AB and Wessberg J. Organization of motor output in slow finger movements in man. The Journal of Physiology, 469: 673–691, 1993.

References

van Hedel H., Tomatis L. & Muller R. (2006). Modulation of leg muscle activity and gait kinematics by walking speed and bodyweight unloading. Gait Posture, 24, 35-45.

Von Hofsten C., Structuring of early reaching movements: a longitudinal study, Journal of Motor Behavior, vol. 23, 1991, pp. 280-292.

Wang, B.Luo, Q. B. Zhang and S.Wei, "Estimation for the number of components in a mixture model using stepwise split-and-merge EM algorithm".

Wiesendanger M. Weakness and the upper motoneurone syndrome: a critical pathophysiological appraisal. In: Berardelli A, Benecke R, Manfredi M, Marsden CD, editors. Motor disturbances II. London: Academic Press; 1990. p. 319–31.

Witkin, A. "Scale-Spacec Filtering", Proceedings of IJCAI, 1019-1021, karlsruhe, 1983.

Wolpert, D. (1997). Computational approaches to motor control. Trends in Cognitive Sciences 1(7).

Woodworth RS. The accuracy of voluntary movements. Psychology Review, 3: 1–114, 1899.

Yang J. & Winter D. (1984). Electromyographic amplitude normalization methods: Improving their sensitivity as diagnostic tools in gait analysis. Archives of Physical Therapy Medicine and Rehabilitation, 65, 517-521.

Yuille A.L. and T.Poggio, "Scale theorems for zero-crossing", IEE trans.Patt.Anala.Machine Intell., vol.PAMI-8, no.1 ,pp 15-25, 1986.

Zollo L, Rossini L, Bravi M, Magrone G, Sterzi S, Guglielmelli E., "Quantitative evaluation of upper-limb motor control in robot-aided rehabilitation", Med Biol Eng Comput. 2011; 49(10):1131-44. doi: 10.1007/s11517-011-0808-1. Epub 2011 Jul 27.

Basmajian J. V., Carlo J. De Luca, Muscles Alive: Their Functions Revealed by Electromyography, Williams & Wilkins; 1985.